UCRL-ID-134409

Advanced Conceptual Design Report for the Z-Beamlet Laser Backlighter System

May 31, 1999

Lawrence Livermore National Laboratory
P.O. Box 808
Livermore, CA 94550

Sandia National Laboratory
P.O. Box 5800
Albuquerque, NM 87185

UCRL-ID-134409

UCRL-ID-134409

Advanced Conceptual Design Report For the Z-Beamlet Laser Backlighter System

May 31, 1998

Prepared for:

Jeffrey P. Quintenz—SNL ICF Program Manager

Approved:

Joseph D. Kilkenny—LLNL ICF/NIF Program Manager

Howard T. Powell—LLNL Laser Science & Technology Program Manager

Stephen A. Payne—LLNL LS&T Associate Program Leader

John A. Caird—LLNL Z-Backlighter Project Leader

UCRL-ID-134409

Acknowledgements

The Z-Backlighter project team wishes to thank all collaborators from Sandia National Laboratories and Lawrence Livermore National Laboratory, whose collective enthusiasm and technical expertise enabled this conceptual design report. We also thank Laser Programs editor Tom Spafford for coordinating multiple review cycles and providing organizational, editorial, and production assistance.

UCRL-ID-134409

Z-Beamlet Laser Backlighter System Advanced Conceptual Design Report

Contributors

Richard Adams (Sandia)
Andy Anderson
Rafael Aragon (Sandia)
Jerry Auerbach
Bill Behrendt
Doug Bloomquist (Sandia)
John Caird
Ellis Dawson (Sandia)
Gary Edwards
Al Erlandson
Jerry Hands (Sandia)
Glenn Hermes
Gregg Holtmeier
Mike Hurst (Sandia)
Harry Ives (Sandia)
Jeff Kellogg (Sandia)
Nino Landen
Barbara Lewis (Sandia)
Israel Martinez (Sandia)
Steve Mills
Jim Murray
Joe Narduzzi
Norm Nielsen
Mary Norton
Charles Orth
John Porter (Sandia)
Jimmy Potter (Sandia)
Andy Seth (Sandia)
Lynn Seppala
Lynn Sheehan
Walt Simpson (Sandia)
Michael Slattery (Sandia)
Stanley Sommer
Jim Spann
Shane Speas (Sandia)
Chris Stolz
Greg Tietbohl
Bruno Van Wonterghem
Colleen Wakefield (Sandia)
Tim Weiland
Richard Zacharias

UCRL-ID-134409

Distribution:

Richard Adams, MS-1188
Bill Behrendt, L-479
Doug Bloomquist, MS-1182
John Caird, L-479
Ellis Dawson, MS-1184
Gary Edwards, L-487
Al Erlandson, L-479
Jerry Hands, MS-1178
Glenn Hermes, L-473
Gregg Holtmeier, L-477
Mike Hurst, MS-1187
Harry Ives, MS-1184
Joe Kilkenny, L-488
Nino Landen, L-473
Barbara Lewis, MS-1192
Israel Martinez, MS-942
Steve Mills, L-482
Jim Murray, L-479
Joe Narduzzi, L-473
Mary Norton, L-479
Charles Orth, L-490
Stephen Payne, L-482
John Porter, MS-1194
Jimmy Potter, MS-1195
Howard Powell, L-482
Jeffrey Quintenz, MS-1191
Lynn Seppala, L-487
Walt Simpson, MS-1194
Michael Slattery, MS-1194
Stanley Sommer, L-495
Jim Spann, L-493
Chris Stolz, L-487
Greg Tietbohl, L-473
Colleen Wakefield, MS-1188
Tim Weiland, L-479
Bruno Van Wonterghem, L-493
Richard Zacharias, L-495

Contents

Figures

Tables

1.0 Summary

The Z-accelerator facility at Sandia National Laboratories (SNL) in Albuquerque, New Mexico, performs critical experiments on the physics of matter at extremely high energy density as part of the Department of Energy's nuclear weapons Stockpile Stewardship Program. In order to augment and enhance the value of experiments performed at this facility, the construction of a new x-ray backlighting diagnostic system is required. New information would be obtained by recording images and/or spectra of x-ray radiation transmitted through target materials as they evolve during Z-accelerator–driven experiments (or "shots"). In this application, we generally think of the diagnostic x-rays as illumination produced behind the target materials and detected after passing through the Z-target. Hence the x-ray source is commonly called a "backlighter." The methodology is a specific implementation of the general science known as x-ray radiography and/or x-ray spectroscopy.

X-ray backlighter experiments have been performed in inertial confinement fusion (ICF) facilities in many countries. On Nova, experience with backlighters has been obtained since about 1986. An intense source of x-rays is produced by focusing one of its beams on a backlighter target nearby, while the other beams are used to create the high-energy-density conditions to be studied in the experiment. This conceptual design report describes how a laser-backlighter similar to one beam of Nova could be constructed for use at Sandia's Z-accelerator facility.

The development of such a facility at Sandia is timely for two major reasons. First, at LLNL the Beamlet laser was decommissioned in FY98, and the Nova laser will be decommissioned in FY99, in preparation for activation of the National Ignition Facility (NIF). This will provide several million dollars worth of subsystems and components from which to construct other lasers, such as the Z-backlighter. Second, the new diagnostic capability at Sandia will provide a national resource for experimentation that would otherwise not exist to complement Nova, and future NIF experiments.

In this report, the primary criteria and functional requirements for an x-ray backlighter diagnostic at the Z-accelerator facility are discussed at the beginning of Chapter 2 (Section 2.1). This is followed by a detailed discussion of subsystem design requirements (SSDRs) for a laser-backlighter that can meet these requirements (Section 2.2). Chapter 3 describes a conceptual design for a laser system that meets these requirements. Chapter 4 provides schedule information for the proposed project. A summary of overall project costs (in FY99 dollars) is shown in Table 1-1.

Table 1-1. Project cost summary.*

Item	Estimated Cost
Facility renovation	$3.6M
Special Equipment	
Procurements	$1.7M
Labor*	$3.6M
Contingency	$1.9M
Total Project	**$10.8M**

* Assumes that labor costs are split roughly 2/3 at LLNL and 1/3 at Sandia.

A management plan for the project including such issues as responsibilities; decision making; environment, safety, and health (ES&H); record keeping; and reporting has not yet been fully detailed. However, a partnership between the LLNL Laser Programs Directorate and Sandia National Laboratories is agreed, with Sandia having ultimate responsibility.

The proposed architecture of the Z-backlighter laser system is almost identical to the Beamlet laser [1], which operated at LLNL from 1995 to 1998 to serve as a scientific prototype for the National Ignition Facility. **Figure 1-1** provides a functional schematic for the Beamlet laser system. This design takes advantage of several technological advances that were not available when Nova was built, and will allow for Z-backlighter performance exceeding that of a single Nova beam with greatly reduced complexity and cost. The development of a full-aperture plasma-electrode Pockels cell (PEPC) [2,3] allows the beam to traverse the main cavity amplifier four times to provide effective use of the gain, as well as efficient use of energy stored in the amplifiers. This feature allows the system to fit into a much smaller space than comparable Nova technology, and enables deployment within space available in Building 986 at Sandia. Efficient frequency conversion (up to 80%) from the fundamental infrared frequency (1ω) to the green (2ω) and ultraviolet (3ω) is accomplished in single, full-aperture (37-cm × 37-cm) KDP and KD*P crystals, compared to the nine aperture-segmented crystal array on Nova). In addition, high beam quality is achieved through active wavefront correction by a deformable mirror (DM) adaptive optic. This has allowed generation of focal spots at the output of Beamlet as small as 3 times the diffraction limit at 1ω [4,5]. A focal spot size this small is a key requirement, enabling high-resolution (4–12 keV) x-ray images to be generated by the Z-backlighter. Key functional requirements for the Z-backlighter laser system are listed in **Table 1-2**.

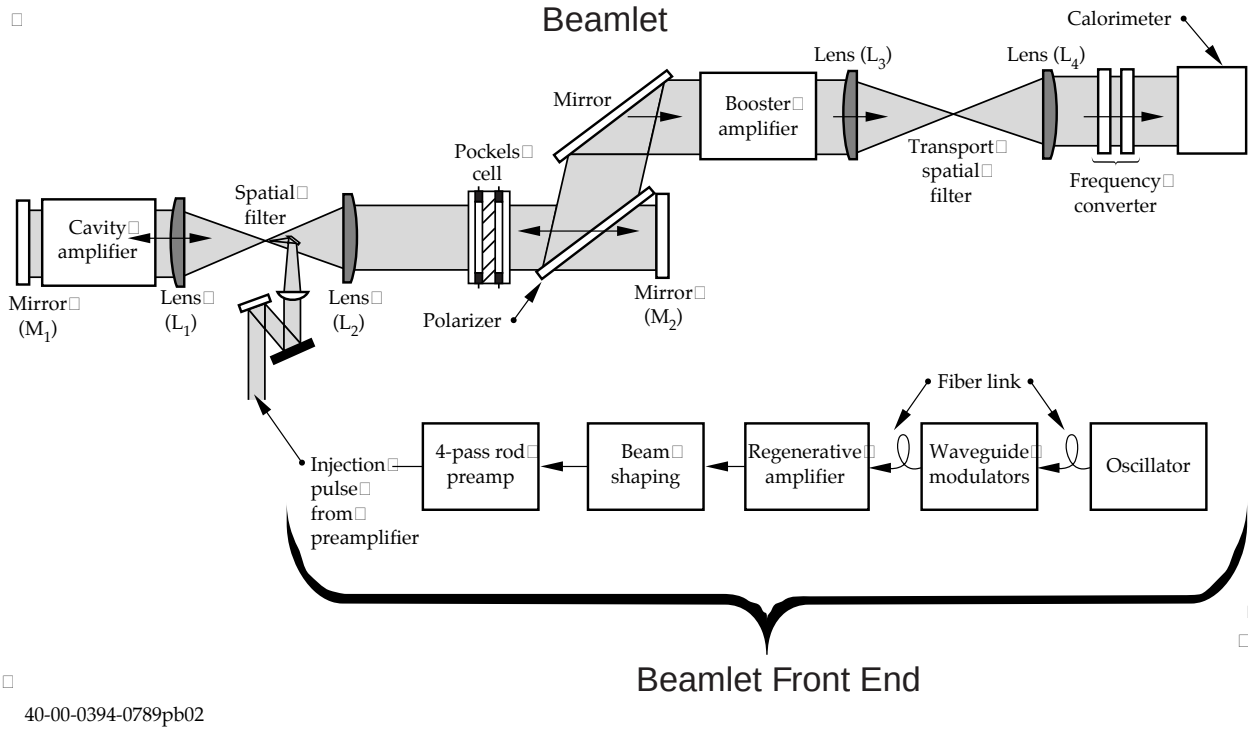

Figure 1-1. Functional schematic diagram of the Beamlet laser.

Table 1-2. Key functional requirements for the Z-backlighter laser system.

Characteristic	Functional Requirement
Laser output energy (2ω, 2 ns)	≥ 2.0 kJ
Focal spot diameter (@ 80% energy)	≤ 50 μm
Irradiance on target*	≥ $3 \times 10^{16} W/cm^2$
Target shot rate	1/day (plus 1 setup shot)
Pulse duration [not to preclude ps operation]	0.2 ns to 2 ns
Temporal pulse format capability	picket fence [up to 4 pulses in 20 ns]

*Temporal peak, spatially averaged over a 50-μm spot

The proposed Z-backlighter laser architecture, shown in **Figures 1-2,** and **1-3**, also employs 4-pass cavity amplifiers with PEPC switch-out, but differs from Beamlet in a number of ways designed to meet mission requirements. Design issues and solutions necessary to meet mission requirements are listed in **Table 1-3**. The main amplifier cavity is shortened from 36 m to 30 m. The cavity amplifiers, C_1 through C_{11}, are Beamlet amplifiers reconfigured from a 2 × 2 to a 1 × 2 square aperture arrangement, and there are no "booster" amplifiers because the output energy requirements are substantially lower than in the Beamlet laser. Room for the Beamlet booster amplifiers is provided for future upgrade of the system, which should not be precluded. Frequency conversion is done following the Beamlet Transport Spatial Filter (TSF), but before the beam is relayed to the target chamber through the 2ω Relay Telescope (2ωRT). This permits mounting the fragile KDP frequency converter (FC) crystal(s) at a sufficient distance from the target chamber to allow them to survive the substantial mechanical shock generated by firing the Z-accelerator. The final 36-m 2ω beam transport is in an argon atmosphere to avoid beam degradation due to Raman scattering in nitrogen. A full-aperture high-damage-threshold 2ω final turning mirror is required to direct the beam into the target chamber. The final focus lens and debris shield assembly must be designed to survive the shock generated at shot time.

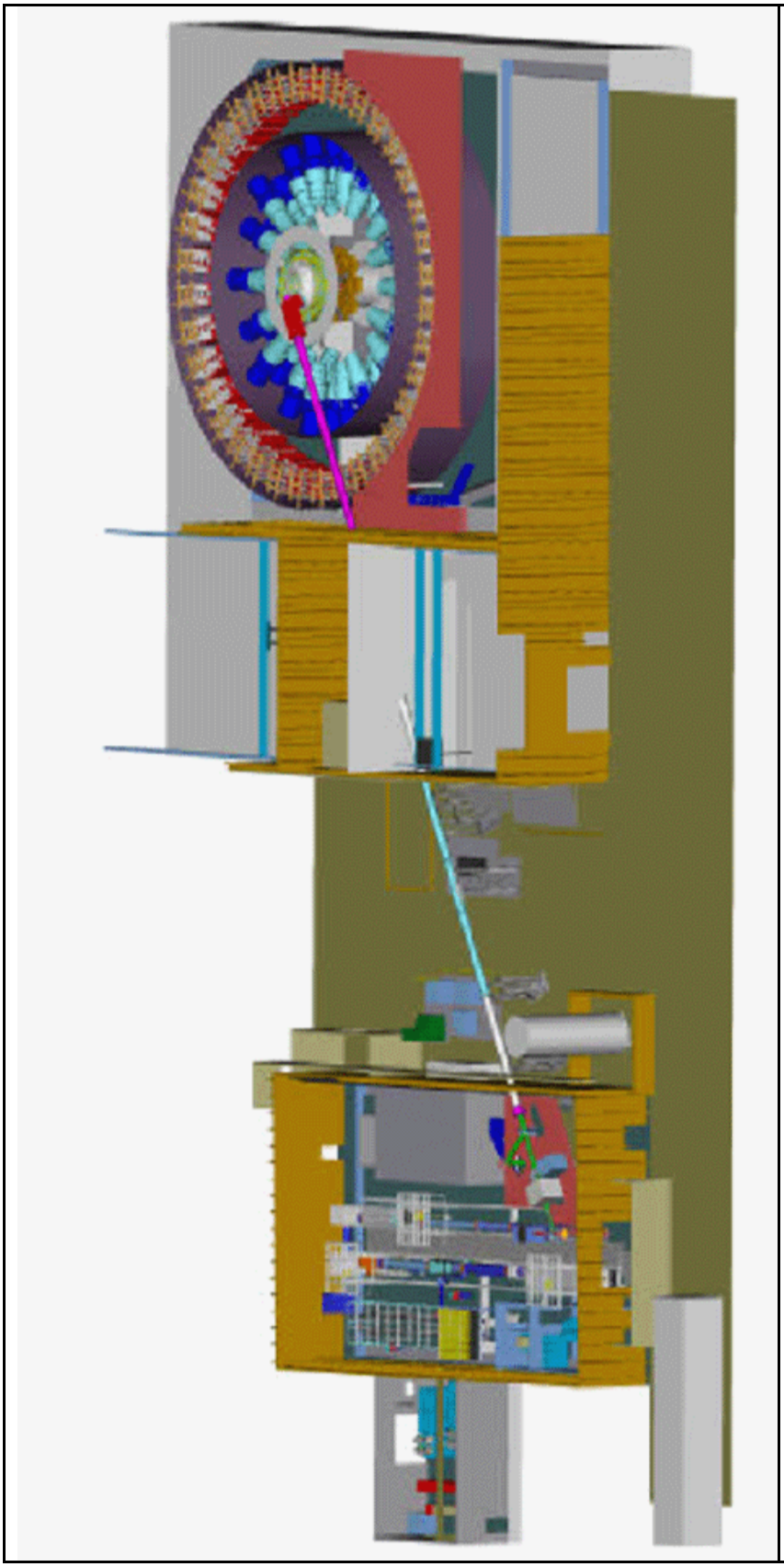

Figure 1-2. Proposed Z-backlighter system layout (view 1). The Z-Beamlet laser facility, Building 986, is shown to the left, and the Z facility, Building 983, is shown to the right.

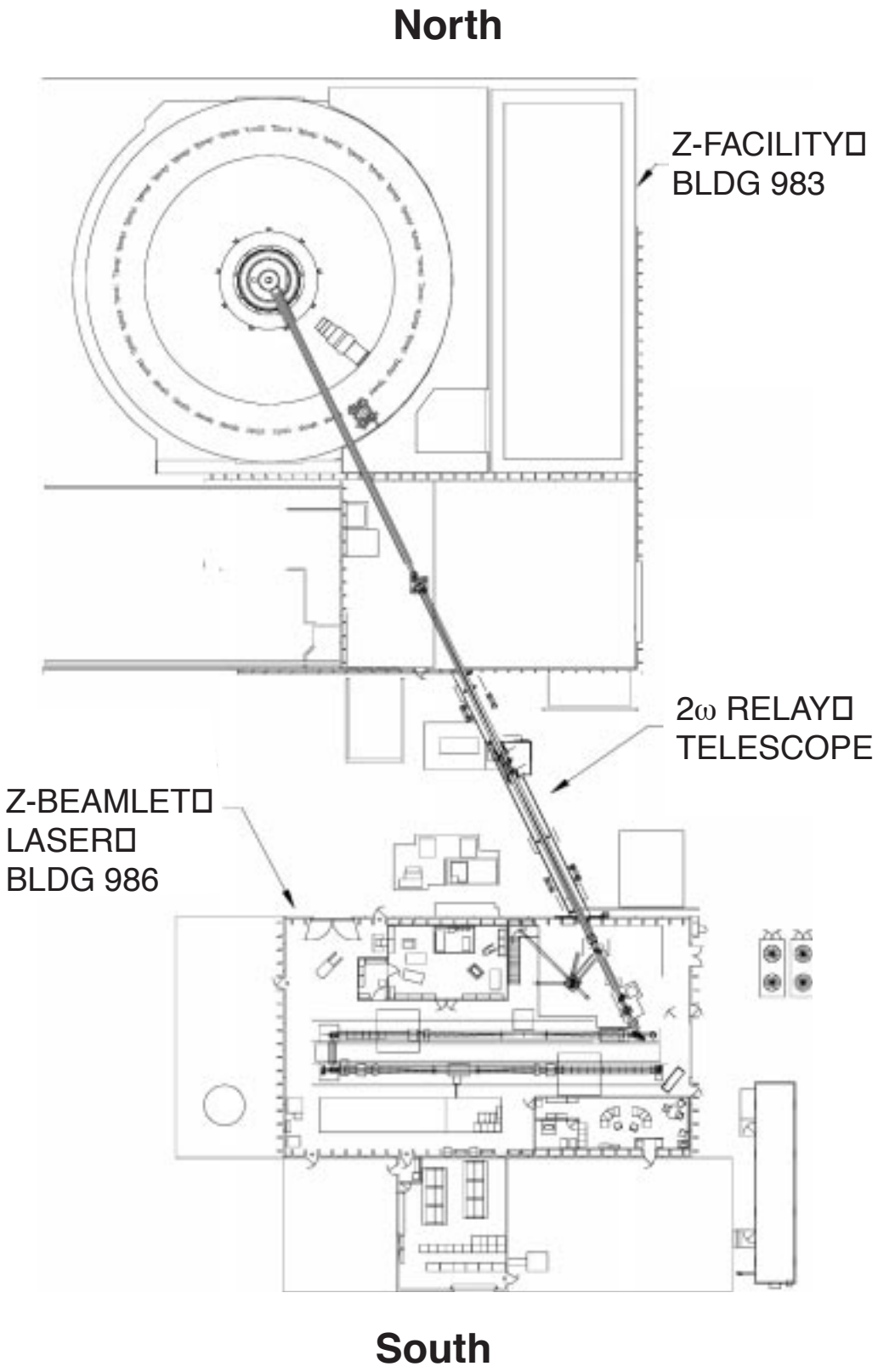

Figure 1-3. Proposed Z-backlighter system layout (view 2).

Table 1-3. Comparison of Beamlet and Z-Beamlet design features.

Item	Design Feature	Beamlet	Z-Beamlet
1	TC mechanical shock	None	Remote frequency conversion, final optics prototype fabrication & test
2	Distance to target chamber	< 1 meter	75 meters
3	2ω propagation	None	2ω relay telescope, argon filled beam tube, minimize 2ω ΣB, robust mechanical stability
4	Minimum pinhole size	150 μrad	200 μrad avoids pinhole closure
5	2ω turning mirror	None	NIF HDT coating technology & online conditioning
6	Master oscillator	Temperature sensitive	NIF style fiber oscillator
7	Synchronization	None	Picket fence pulse generation
8	Regenerative amplifier ring length	10 ns, typical	25 ns, typical
9	Injection optics	Original injection telescope	Redesigned injection telescope
10	Minimize spot size	Deformable mirror	Deformable mirror & low f/# lens
11	Multi-segment amplifier configuration	2 × 2 (dummy glass on inactive side)	1 × 2 (saves bank size and energy)
12	Cavity length	36 m fits in Beamlet high-bay	30 m fits in Sandia's building 986
13	PEPC design	Beamlet prototype	NIF design & performance upgrades
14	Output power & energy	High energy with booster amplifiers	High power without booster amps
15	Frequency converter temperature control	1ω → 3ω requires ± 0.2°C	1ω → 2ω requires ± 0.6°C
16	Output sensors	Complex NIF precision diagnostic	Simplified 1ω and 2ω output beam diagnostics
17	Cleanliness	Class 100,000 high bay, Class 100 clean assembly room	Same, via facility renovation & certification

Most of the special equipment in the Z-backlighter laser system comes from recycled parts from the Beamlet Laser, with some components slightly modified. The entire Beamlet front-end (regen through 4-pass rod preamplifier), shown in **Figures 1-1 and 1-3**, for example, will be reused with only slight modifications. The estimated value of components being recycled for this application is about $6M, the breakdown of which is listed in **Table 1-4**. However, some subsystems, such as the 1ω and 2ω output beam diagnostics, the 2ω relay telescope, and the final optics assembly, are completely new designs for this application. With appropriate modifications, the backlighter proposed here will be transportable to a future facility.

Table 1-4. Breakdown of Beamlet and Nova hardware suggested for use in the Z-backlighter laser—with cost of nearly $6M.

Item	Description	Hardware Value (Thousands of dollars)
Front-end	Existing Beamlet System	1500
M_1, M_2	Beamlet flat mirror, 40-cm clear aperture	100
C_1 to C_{11}	Beamlet 1 × 2 amplifier units (12 each including 1 spare)	1500
Cap Bank	Beamlet power conditioning system	860
L_1, L_2	Recycled Beamlet lens substrates	30
PEPC	Beamlet PEPC, 36-cm clear aperture	300
P	Beamlet polarizers (2)	108
M_3, M_4, M_5	Beamlet bridge mirrors	150
M_8	Nova flat mirror, partially transparent for diagnostics	50
BS	Beamlet beam-splitter, 40-cm clear aperture	30
FC	Beamlet 37-cm x 37-cm KDP frequency doubler	400
L_3, L_4	Beamlet transport spatial filter (TSF) lenses, fl = 9.0 m (3 each including 1 spare)	100
M_9	Flat, ~ 50° angle of incidence, 2ω H/R coating	50
SF	Beamlet spatial filter hardware	100
DFM	Beamlet deformable mirror control system	150
Vacuum system	Beamlet roughing cryo system	75
Align, diag, PC Controls	Beamlet LabView-based system	360
	Total	**$5,863K**

An estimate of the operating costs for the Z-backlighter laser system is provided in Section 3.2.9. The total annual cost of $1.49M includes $840K for labor (including general overhead and floor tax), $150K for operations and optics procurements, and $400K for disposable debris shields.

A substantial part of the project cost—about $4.2M (including contingency)—is required for building 986 facility modifications. These modifications include:

- A new heating, ventilation, and air conditioning (HVAC) system.
- A Class 100,000 clean room environment in the laser high bay.
- A Class 100 clean room environment as an assembly area.
- Concrete piers for improved vibrational stability.

The cost of laser special equipment including detailed design, new and recycled components, control system upgrades, and system activation is $6.6M (including 25% contingency), for a total project cost of $10.8M.

Chapter 4 contains the proposed project schedule. It assumes substantial work in site preparation begins early in FY99. Beamlet components have been shipped to Sandia, and can be redeployed as soon as the new facility is ready. Reactivation of the Beamlet front-end, as well as installation and reactivation of the Beamlet alignment and computer controls systems, will be completed by November 1999. The Beamlet amplifiers, capacitor bank, and spatial filter equipment will be reactivated early in FY00, with final system activation expected by June 2000. An estimate of the funding profile required to complete the project on this schedule is $7.1M in FY99, and $3.7M in FY00. **Figure 1-4** shows the breakdown of the budget estimates into labor and procurements by fiscal year.

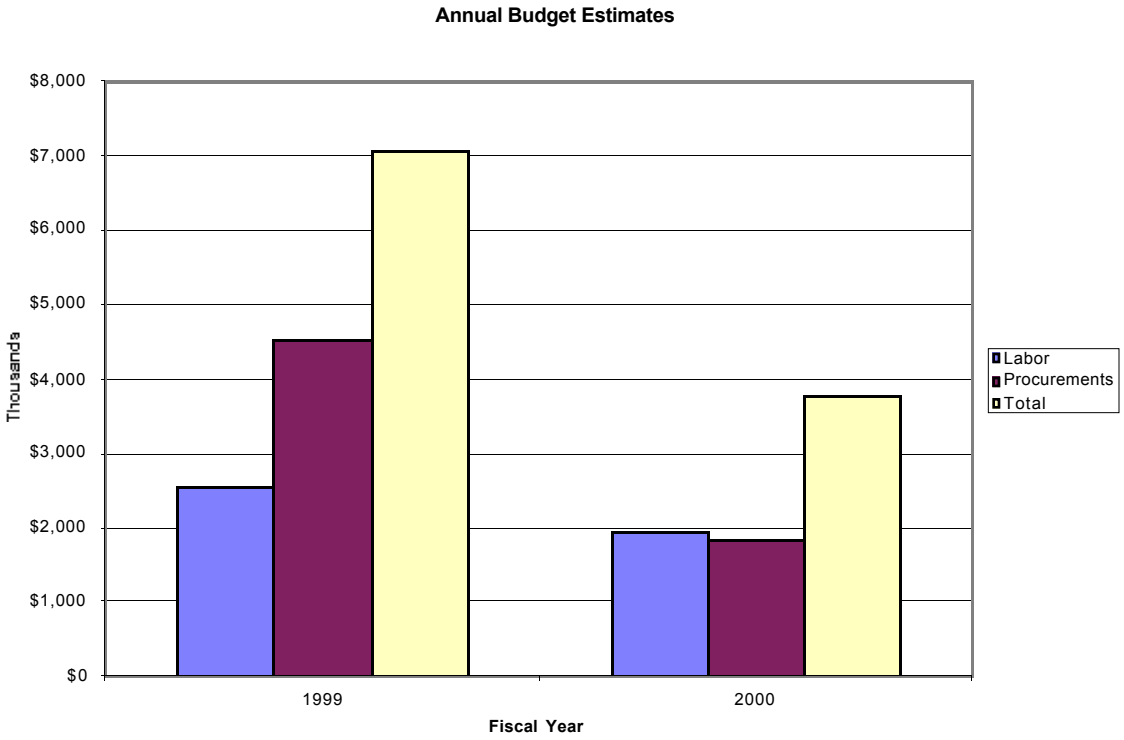

Figure 1-4. Z-backlighter Project annual budget estimates.

2.0 Requirements

2.1 Primary Criteria and Functional Requirements

2.1.1 Primary Criteria

A flexible x-ray backlighting source for diagnosing target dynamics and high-energy-density experiments on the Z-accelerator is required. The x-ray source is envisaged as a kilojoule-class laser plasma with the following laser irradiance criteria:

- Laser wavelength of 0.53 μm (2ω).
- Laser energy of ≥ 2 kJ in a picket fence of ≤2 ns total duration.
- Peak power of 2 TW for pulses <0.5 ns.
- Pointing accuracy of ± 150 μm.
- Irradiance on backlighter target of ≥ 3×10^{16} W/cm^2.
- Irradiance reproducibility of ± 30%.
- >80% of energy in 50-μm-diameter spot size.
- Unconverted 1ω intensity on target <1% of 2ω intensity.
- Pulse duration varying between 0.2 to 0.5 ns in duration (not to preclude picosecond operation).
- Option for up to 4 pulses in 20-ns interval.
- Option of creating smooth, large area (≈1-mm-diameter) spot by inserting phase-plate.
- Option of multiple point foci separated by a few millimeters (with wedged or diffractive optics).
- Option of firing laser between Z-accelerator shots for offline test ("cold shot").
- Option of capturing gated backlit data with < 1-ns timing uncertainty.
- Shot rate to Z-accelerator target chamber of 1/day.

2.1.2 Functional Requirements

Point Projection Imaging

The point projection requirement is for imaging between ≈4–12 keV photon energies at 25-μm resolution. The x-ray photon energy requirements set the laser intensity at 1–30 PW/cm^2. The resolution requirement sets the spot size at (M/(M–1))*25 μm = 50 μm for a standard magnification M = 2. To avoid motional blurring, the maximum acceptable pulse length is between 0.2 and 0.5 ns. To provide multiple snapshots on a single Z-accelerator shot, multiple pulses are required.

For viewing the temporal evolution of sample features that are either 1D, repeating, or random, one can simply gate different segments of a single point-projected x-ray image at different times (see **Figure 2-1**). This allows for a single laser focus.

For viewing the temporal evolution of samples that are 2D or nonrepeating, one needs, in addition to a series of short pulses, spatially distinct point backlighters (i.e., laser foci) for each frame (see **Figure 2-2**). Specifically, for a field-of-view F with magnification M, one requires laser foci separated by at least FM/(M-1), roughly a few millimeters.

Balancing the need for a minimum stand-off detector distance (to avoid detector damage), with the requirement that diffractive and refractive blurring be insignificant, sets the backlighter (and hence laser focus) to Z-pinch distance at ≈1 m.

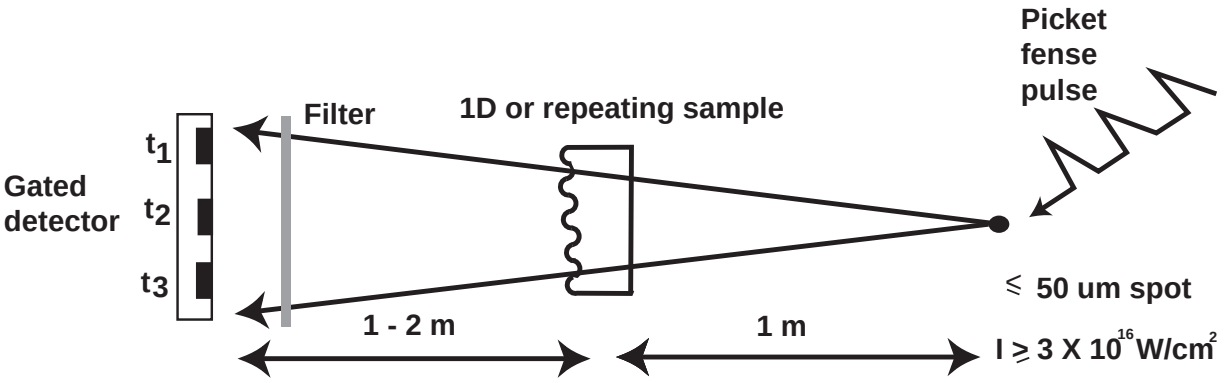

Figure 2-1. Single-point projection backlighting.

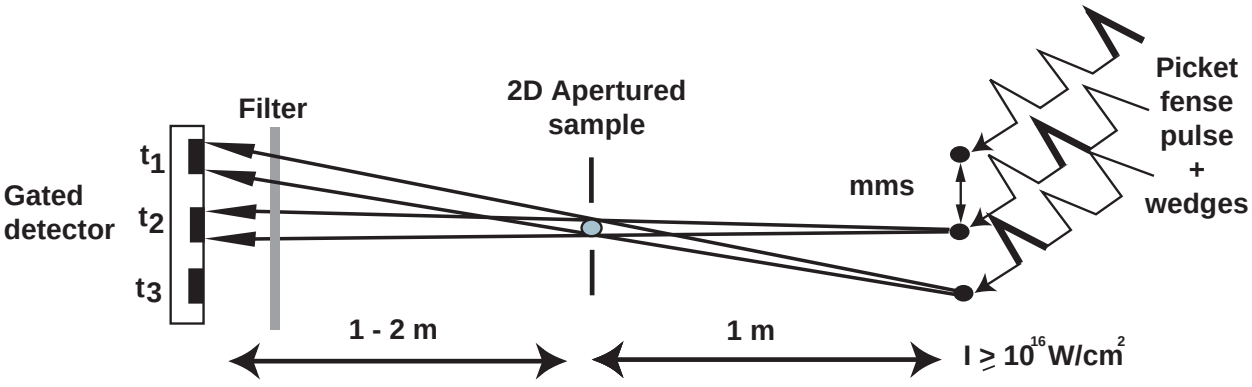

Figure 2-2. Multiple-point projection backlighting.

Area Backlighting

The area backlighting requirement is for 1–3 keV photon energies over approximately a 1-mm spot. A uniform spot of ~1 millimeter can be created by inserting an appropriate phase-plate. An irradiance (power) of 0.1–0.3 PW/cm^2

(1–2 TW total power) is required for creating sources with x-ray energy of 1 to a few keV over this spot size. This mode of operation, however, is not required for the baseline design. The baseline design is not to preclude upgrade to this mode of operation in the future.

For absorption spectroscopy studies, the maximum distance between the backlighter and Z-pinch or experimental package is set by the requirement that the backlighter subtend up to a few degrees angle with respect to the package. This sets the millimeter-size backlighter to package distance at a few centimeters (see **Figure 2-3**). For traditional imaging by pinhole arrays, the parallax between the different lines-of-sight (different pinholes) mandates that the backlighter to sample distance be no more than 1 centimeter.

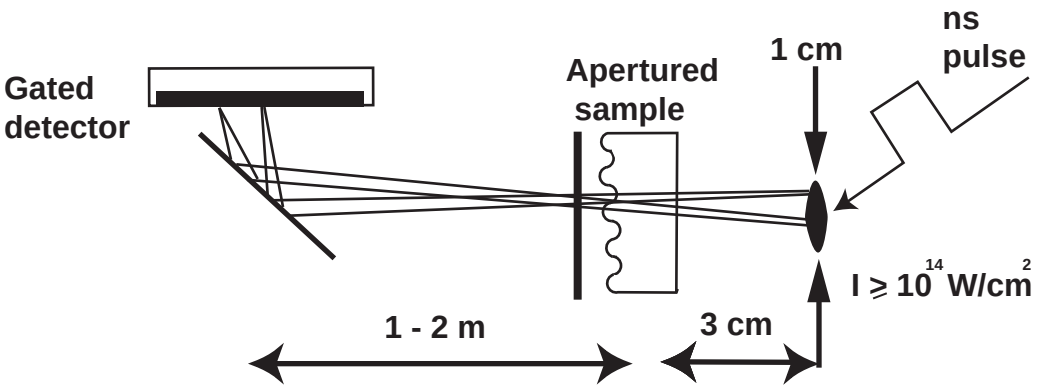

Figure 2-3. Large-area, low-energy (1–2 keV) backlighting.

Timing Jitter

The uncertainty in backlighter timing should be much smaller than the pinch-emission duration of a few nanoseconds. The principal contribution to uncertainty in backlighter timing is expected to be jitter in the pinch emission due to variations in the Z-accelerator pulsed-power switch timing. It is likely that the jitter in Z-accelerator switch timing can be reduced significantly, and this is a recommended course of action in any case. In addition, there are options that can be exercised in laser design and operation to mitigate the effect of accelerator timing jitter. One such approach is described in Section 3.1.

Operations

Two backlighter modes (point-projection and area backlighting) have been identified, requiring separate final optics configurations. The ability to switch between configurations as frequently as monthly would be desirable. The area backlighting option would not be activated during the Z-backlighter implementation initiative.

2.2 Subsystem Design Strategy and Requirements

2.2.1 Laser Architecture and Performance

The Z-backlighter laser architecture is driven by a number of additional constraints. Among these are the following:

- Make the laser system compact enough to fit into the existing facility.
- Provide adequate extraction of stored energy.
- Provide efficient generation of 2ω light remote from target chamber (due to mechanical shock at shot time).
- Use high-quality optics to ensure low wavefront aberration and minimize focal spot size.
- Provide means of correcting pump-induced wavefront distortion.
- Provide flexible temporal pulse-shaping system to create "picket-fence" pulses.
- Design for a robust operation regime to prevent optical damage.
- Utilize a fast final focus lens to minimize focal spot size.
- Provide alignment and diagnostic systems to provide feedback and ensure achievement of performance requirements.
- Minimize laser system and operations cost consistent with meeting design requirements.

The point-projection backlighting mode requires the most stringent beam quality due to the small focal spot size. The laser system must irradiate a target with up to 3×10^{16} W/cm^2 in a focal spot of 50-μm diameter to generate x-rays near 4 to 12 keV that illuminate a secondary hohlraum and a detector with a resolution of ~25 μm. Because of the various types of experiments planned, the x-ray irradiation must be able to span a range of pulse durations from 0.2 to 2.0 ns. Planned experiments impose the following quantitative requirements for the laser:

- Focal spot diameter: 50 μm (i.e., ~3 times diffraction-limited performance for a $\lambda = 1$ μm laser with a beam size of 34 cm and a focal length of 2 m [see Section 3.2.1]).
- Temporal pulse shape: several picket-fence pulses arranged in a cluster or one square pulse.
- Range of pulse durations for a single cluster of pulses: 0.2 to 0.5 ns.
- Number of pulses per Z shot: max. = 4 in 20 ns (total "on time" less than 2 ns).
- Peak irradiance at focal spot: 3×10^{16} W/cm^2 at 2ω (averaged over a 50-μm-dia. spot).
- Energy delivered to the focal spot: 200 J at 0.2 ns, 2.0 kJ at 2 ns (total "on time") at 2ω.
- Reproducibility of irradiance: ±30%.
- Nonlinear phase retardation: ΔB-integral (between pinholes) <2 radians; total B-integral <4 radians.
- Optical damage to components: routine operation at less than 85% of the damage threshold for every component.

- First-to-last photon gain ratio: <35.
- Laser architecture: 4-pass amplifier with PEPC (plasma-electrode Pockels cell) switch-out using a polarizer (for compactness and efficiency).
- Pointing accuracy: ±150 μm.

2.2.2 Optical Design and Ghost Control

Existing Beamlet and Nova components will be reused whenever possible to reduce cost. Clear aperture size must be consistent with optical damage thresholds and required output power and energy. Multipass cavity pinhole spacing must be consistent with required beam size and pass-to-pass vignette. Component spacing must be consistent with benign location of ghost foci within the optical train (ghosts are unavoidable reflections from optical surfaces; they can damage components if allowed to focus at vulnerable locations). **Table 2-1** contains a preliminary estimate of the Beamlet and Nova large optics that will be reused or reworked into new components. Some sizes, shapes, and thicknesses will change later as the design evolves.

Table 2-1. Estimated re-allocation of Beamlet/Nova large optics for Z-Beamlet.

Z backlighter designation	LLNL part number	Tab #	S/N	Beamlet designation	Current size (cm)	Reworked size (cm)	CenTh (cm)	Shape	Comments: rework or purchase
Z-BEAMLET									
M1	91-110120	t 01	sn 01	M-1	61		8	round	
C1-C11	91-110113			main cavity amplifier	44.8 x 77.8		4	rectangle	
L1 **(rework)**	94-101364	t 02	sn 11	L-1	44 x 44	44 x 44	4.6	square	**rework to f=7.5 m**
L2 **(rework)**	94-101364	t 02	sn 03	L-2	44 x 44	44 x 44	4.6	square	**rework to f=7.5 m**
PEPC-W1	91-110114		sn 01	Pockel cell window	41.4 x 41.4		3	square	
PEPC-KDP	91-107622	t 07	368-2	Pockel cell KDP	37 x 37		1	square	
PEPC-W2	91-110114		sn 03	Pockel cell window	41.4 x 41.4		3	square	
POL	91-100522	t 01	sn 04	Polarizer	45 X 78		9	rectangle	
M2	91-110120	t 02	sn 01	M-2	61		8	round	
M3	91-110120	t 03	sn 01	M-3	65.5		7.8	round	
M4	91-110120	t 03	sn 02	M-4	65.5		7.8	round	
M5	91-100522	t 01	sn 03	M-5 Polarizer	45 X 78		9	rectangle	
B1	91-110113			booster amplifier	44.8 x 77.8		4	rectangle	
L3	95-101057	t 02	sn 05	L-3, tilted	44 x 44		4.2	square	
L4	94-101364	t 02	sn 04	L-4	44 x 44		4.6	square	
M6	91-110120	t 03	sn 03	mirror:M3-M4 spare	65.5		7.8	round	
M7	91-110120	t 03	**rework**	**78-115226-OH tab06b**	**94**	61	12	round	**Nova rework**
M8	new		**rework**	**78-115225-OH tab06**	**94**	44 x 78	10	rectangle	**Nova rework**
FC	91-107622			2w freq converter	37 X 37		1.1	square	
2wBS	92-105476	t 05	sn 06	1w splitter	61		3.5	round	
L5	new		**rework**	**78-117095-OF tab06a**	**94**	44 x 44	5.7	square	**Nova rework**
L6	new		**rework**	**78-117095-OF tab06a**	**94**	44 x 44	5.7	square	**Nova rework**
CAL									
M9	new		**rework**	**78-115226-OH tab06b**	**94**	44 x 78	12	rectangle	**Nova rework**
FF1	new		**new**			38 x 38	5.5	square	purchase
DS1	new		**new**			30.5	2.5	round	purchase

Optical Coatings

Optical coatings are necessary for the spatial shaping, polarizing, and steering of the Z-backlighter laser beam. These coatings can limit the laser fluence due to the optical damage threshold of the coated surfaces. Optical components also limit the laser beam transport efficiency by their spectral reflectivity or transmission. The final wavefront of the laser beam is impacted by the optical surfaces and material homogeneity, which influences the focusability of the laser beam.

General requirements for large-aperture optical components include:

- Minimal wavefront distortion (in waves p-v).
  —<λ/2 polarizers, <λ/3 all other optics.
- Optical components shall have damage thresholds in excess of 15% greater than the peak laser operating fluence.
- Peak vacuum-induced stress loads of less than 500 PSI to ensure that catastrophic failures due to rupturing will not occur.
- Minimal transport loss due to interaction with the optic.
  — Transmission >99.5% an all windows, crystals, and lenses.
  — Reflection >99.5% on all mirrors.
  — Reflection at "S" polarization >99.5% on the cavity polarizer.
  — Transmission at "P" polarization >98% on the cavity polarizer.
- Control of ambient humidity is required to maintain specified performance of some multilayer coatings.

2.2.3 Mechanical Systems

Mechanical systems are defined as the special equipment necessary to support the optics and maintain the proper atmosphere around them. This is distinct from the conventional facilities, which include building foundation work, HVAC, cooling water, and clean rooms.

The primary requirement for the mechanical systems is to house and position all the optical elements. This must be done in a manner that meets the pointing stability specifications for each optic that is supported. In addition, the optical enclosures must prevent unwanted laser breakdown and degradation through the use of vacuum enclosures for the spatial filters and inert-gas-filled enclosures within the laser cavity to prevent tarnishing of silver reflectors. Mechanical systems must be designed to accommodate laser refurbishment, as well as the daily operations in the Z-accelerator facility.

A special requirement in the final optics area (last turning mirror(s), focus lens, vacuum window, and debris shield) is to mount the optics such that at most only the debris shield is damaged by the shock and debris generated by the Z-pinch event. There can be no catastrophic loss of vacuum to the Z-pinch chamber. The final optics package must be removable after each accelerator shot which occurs on a near daily basis. The detailed requirements for this equipment will be determined in a risk-reduction or advanced design phase.

2.2.4 Laser Alignment and Diagnostics

Alignment

Alignment capability consists of the ability to center and point the beam at each location along the beam path where there is the potential for misalignment, for example after one or more beam transport mirrors. Not all such locations need to be addressed during routine alignment, and not all need to be remotely accessible, but the capability must exist at all locations to manipulate beam position and direction.

Centering refers to the transverse positioning of the beam at a given location, and the centering requirement is to position the beam within 1% of its diameter. *Pointing* refers to the direction of the beam in horizontal and vertical planes, and the pointing requirement is ±50 μrad in both planes for sufficiently accurate alignment to ±200-μrad pinholes.

Efficient harmonic generation requires orientation of the KDP crystal to within ±160 μrad (assuming the 1.1-cm-thick Beamlet KDP Type I doubler crystal), which gives greater than 95% of the theoretical peak conversion efficiency. The most stringent target alignment requirements are for the point backlighter targets. In that case, the target must be positioned to within ±0.15 mm in the transverse directions, and the 2ω output beam must be focused to a spot size on target less than 10% greater than the minimum possible.

The alignment approach should be as close as possible to that which was successfully employed on the Beamlet laser. The procedure is manual, in the sense that an operator determines if corrections are required, usually from video data, and implements the corrections by manipulating mirror tilts, translation stages, etc. Most of the information for the operator to make alignment choices, and the controls for manipulating the requisite hardware, will be available at one of several consoles.

Diagnostics

Diagnostics must make it possible for the operators to tell if the laser is functioning properly and if enough second-harmonic power is generated to drive targets as required. In the following set of required laser diagnostics, most of the near- and far-field detectors must span a large enough sensitivity range to cover system shots, front-end shots, as well as alignment with a continuous wave (CW) laser:

- Regen output: near field, far field, and power.
- 4-pass rod input: near field, far field, energy, and back-reflected power
- 4-pass rod output: near field, far field, power, and energy.
- 1ω output: near field, far field, energy, and power, and wavelength.
- 2ω output: near field, far field, energy.

Wavefront Control

In order to achieve a high-resolution x-ray image, it is important that the focal spot of the laser be small. The goal for this system is to achieve a spot size that is 50 μm in diameter (approximately three times the optical diffraction limit at 1.06 μm).

Aberrations in the laser optical system may preclude achieving the required spot size without wavefront correction. Primary sources of correctable aberration include pump-induced thermal aberrations in the laser slabs, optics figure errors, coating-induced stresses on optics, mounting-induced stresses on optics, gravity sag on non-vertical optics, alignment, off-axis beam-induced aberrations, and residual thermal aberrations from previous shots, etc. Dynamic aberrations induced by gas density

variations may also be corrected with the addition of a fast-actuator system to quickly change the system state from wavefront control to shot-ready. Beamlet includes such a fast actuator system.

The Beamlet laser has achieved the required level beam divergence using a deformable mirror wavefront correction system. The Z-Backlighter laser will require a similar wavefront correction system.

2.2.5 Power Conditioning

The Z-Beamlet power conditioning system will use switching power supplies to charge the pulse-forming and energy-storage capacitors. The stored energy will be discharged into flashlamps in the 11 main amplifiers, rod amplifier and Faraday rotator. Ignitrons will be used as the high-energy switch. All components will be reassembled as they were configured in Beamlet.

The power conditioning room should be constructed of a material that will contain any components in the event of failure and be equipped with a safety interlock system to prevent operation of the system unless all safety systems are functional. The ignitron switches will require additional continuous water cooling to maintain internal liquid mercury at or near 25°C. Additional anode heating is also required to maintain the anode element at or near 100°C. The total energy storage will be on the order of 5 MJ.

2.2.6 Control System

A brief summary of functional requirements for the Z-Beamlet control system (ZCS) is as follows:

- Coordinate shot setup, including laser alignment, power conditioning, timing sequence control, countdown, and shot laser diagnostic data archiving.
- Provide graphical operator controls and equipment status.
- Maintain records of system performance and operational history.
- Incorporate safety and equipment protection interlocks into the Z-accelerator Access Control System.
- Provide remote access to the laser control system from the Z-accelerator control room.
- Provide interface and shot synchronization with the Z-accelerator Control/Monitor (C/M) System.

ZCS performance requirements:

- Respond to broad-view status updates < 10 seconds
- Respond to alerts < 1 second

2.2.7 Frequency Conversion

The frequency converter subsystem is required to:

- Convert the output wavelength of 1.053 μm to 0.527 μm.
- Provide a clear aperture of ≥ 34 cm × 34 cm.
- Operate with high conversion over a range of 2.5 GW/cm^2 to 3.5 GW/cm^2. (for example: for a 1-ns pulse 70% peak conversion to provide 2 kJ at 0.527 μm.)
- Provide a controlled environment for the frequency converter crystal(s) to produce efficient conversion, prevent optical damage, and prevent degradation, which includes:
  - temperature control to ± 0.6°C.
  - particulate control.
  - humidity control.
- Fit in a space 5-ft long in the beamline direction, 6-feet tall and 6-feet wide.
- Provide remote tuning of the converter crystal (or crystals) to maintain alignment of tuned crystals to ±160 μrad (external angle) to maintain converted output energy repeatability for a given input to ±5%.
- Provide a useful alignment beam with input from the regenerative amplifier.
- Minimize wavefront distortions to allow the converted output to be focused to a 50-μm spot with a 2-m focal-length lens.

2.2.8 Site and Conventional Facilities—Requirements

The Site and Conventional Facilities work for this project will involve the modification of Building 986 to accept the backlighter laser and support equipment, and installation of special equipment in Building 983. Both buildings are in Technical Area 4 at Sandia National Laboratories in Albuquerque, New Mexico. Building 986 is classified as approximately 9800 square feet of high bay laboratory space with some office, restroom and storage functions. The Z Accelerator resides in the high bay of Building 983, which is located approximately 70 feet north of Building 986.

General design considerations for all modifications to the site must follow the most recent issue of the regulatory requirements and standards listed herein. Conflicts among documents will be resolved by employing the most stringent requirements or by presenting the conflict to the Backlighter Installation Configuration Control Team for resolution. In all cases, design will be in accordance with DOE Article H-37 Life Cycle Asset Management (LCAM) Requirements.

- American National Standards Institute/Instrument Society of America, ANSI Y32.20, Instrumentation Symbols and Identification
- American Society for Heating, Refrigeration and Air Conditioning Engineers (ASHRAE), Guideline 1-1989, Guideline for Commissioning of HVAC Systems
- ASHRAE Standard 62, Ventilation for Acceptable Indoor Air Quality
- American Society of Civil Engineers, ASCE 7-95, Minimum Design Loads for Buildings and Other Structures
- Americans with Disabilities Act (ADA)
- Checklist of Hazard Factors for Facility Design and Operation
- DOE Order 5700.2C, Cost Estimating
- DOE Protected Distribution System (PDS) Manual, 4-1-94

- DOE-STD-1020, Natural Phenomena Hazards Design and Evaluation Criteria for Department of Energy Facilities, as revised for ASCE 7-95
- Insulated Cable Engineers Association (ICEA) Standard ICEA-S-68-516, Ethylene-Propylene-Rubber-Insulated Wire and Cable for the Transmission and Distribution of electrical Energy
- National Electric Code (NEC)
- National Fire Protection Association (NFPA) 780, Lightning Protection Code
- NFPA 13, Standard for the Installation of Sprinkler Systems
- NFPA 72, National Fire Alarm Code
- NFPA 101, Life Safety Code
- Occupational Safety & Health Act (OSHA) Standards (29CFR1910)
- SNL Gowning Procedures, Version 6.0
- Steel Deck Institute, Roof Deck Design Manual
- Steel Joist Institute, Standard Specification for Open Web Steel Joists
- Uniform Building Code (UBC)
- Uniform Fire Code (UFC) and NFPA 70

In addition, the following specific internal building criteria will be incorporated into the design:

- Broadband ambient vibration for 1 to 200 Hertz = 1×10^{-9} g^2/Hz.
- Internal temperature control = 68°F ± 1°F (from the bottom of the lower beam tube to the top of the upper beam tube).
- Tolerate levels of acoustic vibrations, which must be determined during design.
- Class 100,000 and Class 100 clean room areas.
- Dynamic excitations from experimental shots ≤ 0.05 g

2.2.9 Laser Operations and Start-up

During routine operations, the Z-backlighter laser is required to fire a minimum of one shot per day in a safe and cost-effective manner. A second shot for calibration of sensors, alignment offset measurements, or other offline laser experiments must also be available. Appropriate staffing and funding will be required to ensure this type of operation.

Staffing requirements consist of personnel to support laser system operations and maintenance. This includes technicians trained in laser electro-optics to support laser alignment, integrated system operation, and laser hardware maintenance. Maintenance includes tasks such as amplifier refurbishment, optics cleaning and installation, and optics characterization. Technicians trained in electronics, mechanical, and computer systems will also be required to support system maintenance, such as power-conditioning repairs, vacuum system maintenance and repair, and computer controls and data acquisition maintenance and repair. Additionally, this type of high-power laser system and some support areas must be maintained in a technically clean environment. Cleanliness at this level requires dedicated custodial support.

Adequate funding is required to maintain the system in a safe and efficient operating condition. This includes spare equipment such as amplifier flashlamps, optical components, maintenance contracts to support alignment lasers and software, clean room supplies, electronics subsystem spares, etc.

Many of the components used in this laser system are custom parts built and maintained by LLNL. These components are not available "off the shelf" from commercial vendors. There will need to be the ability to fabricate, assemble, and test some of these components. This includes items such as diode-mounting fixtures used in power conditioning, special assembly fixtures, vacuum test fixtures, etc. In general, LLNL has drawings and specifications for these systems, but support for replacement fabrication, modification, and maintenance will need to be provided. It is the intent of LLNL to support the Z-backlighter operations with its ICF infrastructure with direct cost charge, as required.

Additional personnel support will be required during system activation and start-up. This will include additional laser technicians to support hardware assembly, installation, and alignment. Additional mechanical and electrical technician support will also be required to install power-conditioning hardware, control and data acquisition systems, and mechanical components. The need for additional support will decline rapidly after the first several months of operation.

3.0 Conceptual Design

3.1 X-Ray Backlighter Target

Backlighter targets are envisaged as being a few mm-thick, cm-diameter foils of mid to high Z materials. The minimum thickness is set by the requirement of delaying foil acceleration (i.e., displacement) and decompression during multiple pulse irradiation. Acceleration and eventually decompression occurs after the laser-produced shock transits the foil. For example, at irradiances of 10 PW/cm^2, shock speeds of up to 100 μm/ns are expected. For the most conservative calculation based on planar shock propagation, this sets the minimum foil thickness at 2 mm if foil acceleration is to be delayed over the maximum 20-ns backlight duration.

3.1.1 Point Projection Imaging

The decision to use a large area foil rather than a fiber of subfocal spot size dimensions as backlighter target for point-projection imaging is based on the following:

1. The x-ray spot size as set by the laser focus size provides adequate resolution.
2. The full focal spot (i.e., full power) of the laser is used to create x-rays.
3. The pointing accuracy requirement is greatly reduced (from ≈30 to 150 μm).
4. A thin-fiber target could not accommodate multiple pulse irradiation over many nanoseconds.
5. If plasma expansion did lead to unacceptable source broadening and reduction in spatial resolution, then pinhole arrays inserted between the "point" backlighters and sample of interest could be used to limit the maximum source size.

For point projection imaging between ≈ 4–12 keV photon energies, standard laser plasma sources consisting of K- and L-shell resonance lines of highly stripped mid-Z and high-Z elements (respectively) are envisaged. The longer pulses (> 0.2 ns) are required to match the ionization times for stripping some of the higher-Z elements to the appropriate charge state. The x-ray backlighter efficiency at relevant laser wavelengths, pulse-lengths, and intensities has been measured recently for three target materials (Ag [3 keV], Zn [9 keV] and Au [10 keV]) at the Nova and Omega facilities. The x-ray conversion efficiencies support earlier estimates of brightness and hence validate the notions that the detected number of photons per resolution element will provide adequate photon statistics.

For minimizing spot size and optimizing coupling between the laser and the backlighter foil target, the incidence angle should be within 30° of normal incidence. This has the added advantage that the maximum allowable transverse mispointing of 150 μm translates into < 100 μm defocus error at the backlighter target surface, less than the Rayleigh range. In addition, the x-ray viewing axis should be no less than 30° from

an edge-on view of the foil. This ensures that cratering of the foil due to a previous pulse does not lead to vignetting of the x-ray emission from succeeding pulses.

The x-ray source size broadening due to plasma expansion along the laser axis during point-projection imaging has been measured at the Nova facility at the relevant intensities and pulse lengths. The results indicate a plasma expansion velocity of 100 μm/ns normal to the target surface, and negligible transverse expansion. Since the maximum point source duration is set at 0.5 ns, the expanded source size viewed edge-on will be no greater than the intrinsic design footprint of the beam (50 μm). Hence, there is no additional restriction set by expansion on the angle between the target normal and x-ray viewing axis. If spatial wings outside the 50-μm spot size are deemed problematic, then a 50-μm pinhole set between the backlighter and sample can be used to clip these wings. The minimum angle between the laser and viewing line-of-sight will probably be set by the need to shield the final focus assembly from a direct view of pinch debris.

3.1.2 Area Backlighting

Both broadband and monochromatic backlighter sources will be needed in the future for area backlighting. For 1–2 keV broadband sources, irradiating high-Z foils such as uranium yields a near Planckian spectrum at a few hundred eV temperature. For broadband sources between 2–4 keV, M-shell line arrays from high-Z elements are commonly used. Monochromatic K and L shell line sources at a few keV are readily available by irradiating low-Z and mid-Z elements respectively. In cases where two discrete photon energies are required, the backlighter foil may consist of a mixture of two elements, either cosputtered or placed side-by-side.

The angle between laser axis, x-ray viewing axis and backlighter target normal is less critical for area backlighting. However, a maximum laser incidence angle of $\approx 30°$ is recommended for maintaining good laser-foil coupling efficiency. In addition, the requirement that the area backlighter be only a few cm from the pinch or sample of interest may set the minimum angle between laser and x-ray viewing axis.

3.1.3 Mitigation of Timing Jitter

More stringent timing jitter demands are being placed on the Z accelerator as the x-ray emission pulse widths are decreasing to ~5 ns. Several accelerator components contribute to the overall system jitter, and consideration of possible jitter reductions must include cost, operations impact, and shot schedule.

Historically, the principal contributor to accelerator jitter has been the jitter (here defined as the one standard deviation of the timing measurements relative to their mean) associated with the Laser Trigger System (LTS) excimer laser used to optically trigger electrical conduction of pulsed power through each of the 36 high-voltage gas switches. Figure 3-1 reveals the jitter performance of the entire accelerator and that of the excimer laser itself over a number of shot groups (each containing 8 to 30 shots)

spaced over many months for a given type of wire array load. The accelerator timing was determined by an average of electromagnetic sensors (B monitors) situated in the final transmission lines with a 10% level-crossing for the typical ~20-ns rise time pulse shapes. The laser timing was determined by the 10% level-crossing for the ~5-ns rise time of the KrF laser pulse.

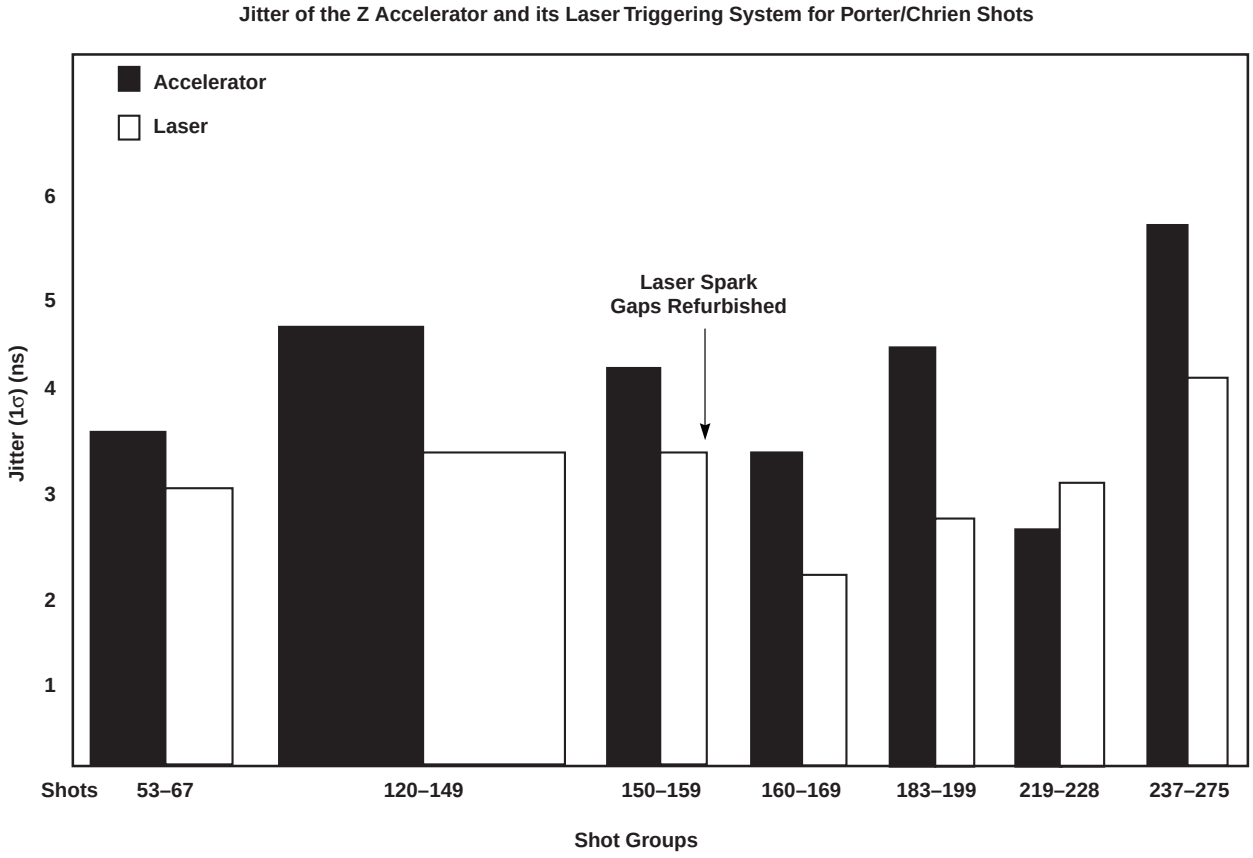

Figure 3-1. Jitter performance of the entire accelerator and of the excimer laser over a number of shot groups for various wire array loads.

Figure 3-1 indicates that most of the accelerator jitter does originate with the excimer LTS laser, keeping in mind that jitter components add in quadrature. Most importantly, from the figure it is apparent that the laser jitter consistently increased with shot accumulation until the laser spark gaps were refurbished, thereby decreasing laser jitter by 1 ns. With continuing use (the LTS laser is fired about twenty times prior to every accelerator shot) following refurbishment, the laser jitter rose significantly. This data implies that under optimal conditions, this LTS laser could exhibit ~2-ns jitter and the entire accelerator ~3–4-ns jitter.

Another significant accelerator jitter source involves the behavior of water switches, which are self-breaking switches located in the water section downline from the laser-triggered gas switches. From Figure 3-1 and other databases, the water switches exhibit

~2-ns nominal jitter but can degrade due to mechanical shock if not frequently inspected.

An additional jitter contribution arises from the z-pinch behavior itself relative to x-ray emission and constitutes ~1-ns of jitter, being dependent upon the repeatability of wire array mass, dimensions, and other parameters.

Several options for accelerator jitter reduction are possible. First, the excimer laser spark gaps could be refurbished more frequently, e.g., every month instead of the present yearly interval. Spare spark gaps are relatively inexpensive, and the change-out time requires less than four hours. Second, the laser spark gaps are triggered by a commercial hydrogen thyratron with ~1-ns jitter and a one-year replacement interval. This thyratron behavior could be closely monitored for jitter degradation, prompting earlier thyratron replacement. Next, all 36 water switches could be inspected before every accelerator shot, at least on a trial basis, to see if the improved water switch jitter warrants the additional labor costs and shot delays compared to the present 9 switch inspections per shot. Finally, the most dramatic and costly option would involve replacing the existing excimer LTS laser with a solid-state ultraviolet laser having comparable gas switch triggering performance but subnanosecond laser jitter. This change would require careful planning to avoid disrupting accelerator shot schedules and would involve extensive optics replacements.

If one or several of these jitter mitigation options are implemented, the Z accelerator will probably still exhibit timing jitter of 2 ns or more. This conclusion implies that the backlighter laser must still consist of multiple pulses (the "picket fence") in order to ensure backlighter data on every accelerator shot (see below). The key advantage realized by accelerator jitter reduction is that the total width of the picket fence and hence backlighter laser complexity can be reduced.

The mitigation of z-pinch timing jitter by use of a "picket fence" pulse train can be quantified as follows. Consider the effect of a jitter of $\pm \Delta t$ ns on backlighter timing relative to a particular event on the pinch (e.g., peak emission time). If only a single laser pulse and frame were available, this would translate to a shot-to-shot timing deviation of up to $\pm \Delta t$ ns. By using multiple pulses and frames spaced Δt ns apart, the root-mean-square (rms) timing deviation relative to the peak emission time is reduced by a factor of $2\sqrt{3} \approx 3.5$, as shown in **Figure 3-2**. For a typical jitter Δt of $\pm$ 2 ns for the Z-accelerator, this equates to an rms timing deviation of only 0.6 ns. This is much shorter than the FWHM duration of the pinch emission (> 4 ns), as required.

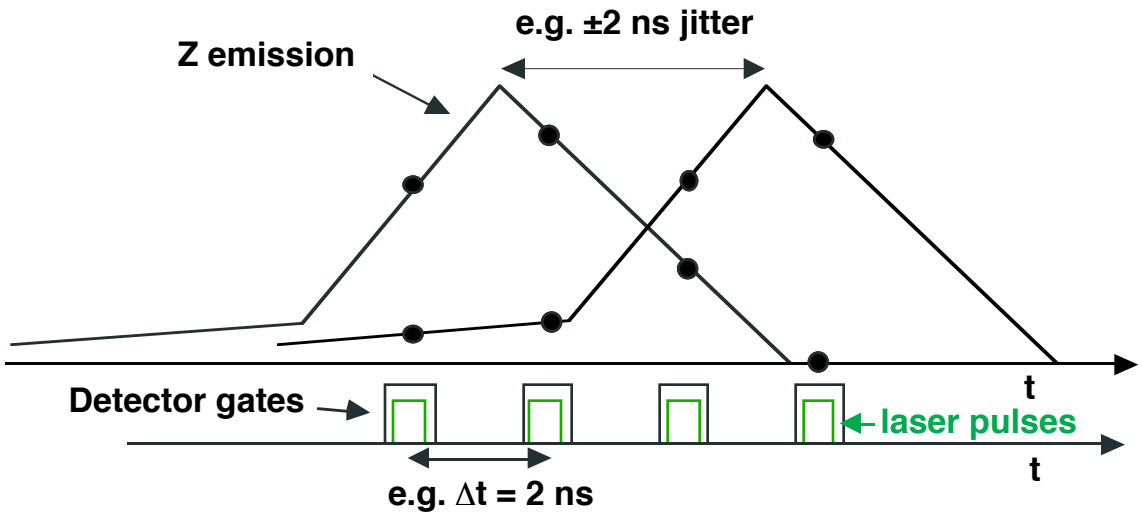

Figure 3-2. Mitigating timing jitter – example using multiple frames.

3.2 Laser Subsystem

Refer to Figure 3-3 to identify laser subsystem components described in this section.

3.2.1 Laser Architecture and Performance

Laser Architecture

As mentioned in Chapter 1, the Z-backlighter laser system is very similar to Beamlet with minor modifications. In fact, the Z-backlighter laser will be built almost completely using recycled components from Beamlet. Key changes in the design are listed in **Table 1-3**, and include addition of a new master oscillator, reduction of the cavity spatial filter length, deletion of the booster amplifiers (because backlighter experiments typically require much less energy than Beamlet was originally designed to produce), deletion of the KD*P frequency tripling crystal, addition of a 2ω relay telescope for beam transport to the target chamber, and addition of a final beam focusing system at the target chamber. A phase modulator can be readily added for long-pulse shots requiring suppression of SBS in the final optics. Facility modifications will be made to provide adequate mechanical and thermal stability for the Z-Beamlet laser. The Beamlet temporal pulse-shaping system will be augmented with new fast-pulse generators, amplifiers, and delay generators as needed to produce up to 4 pulses in a 20-ns picket fence. Frequency conversion is done remotely from the target chamber so that the fragile KDP frequency converter (FC) crystal(s) are able to survive the substantial mechanical shock generated by firing the Z-accelerator. A full-aperture 2ω final turning mirror is required to direct the beam into the target chamber. Plan views of the Z-Beamlet laser system are shown in **Figures 1-3 and 3-3**.

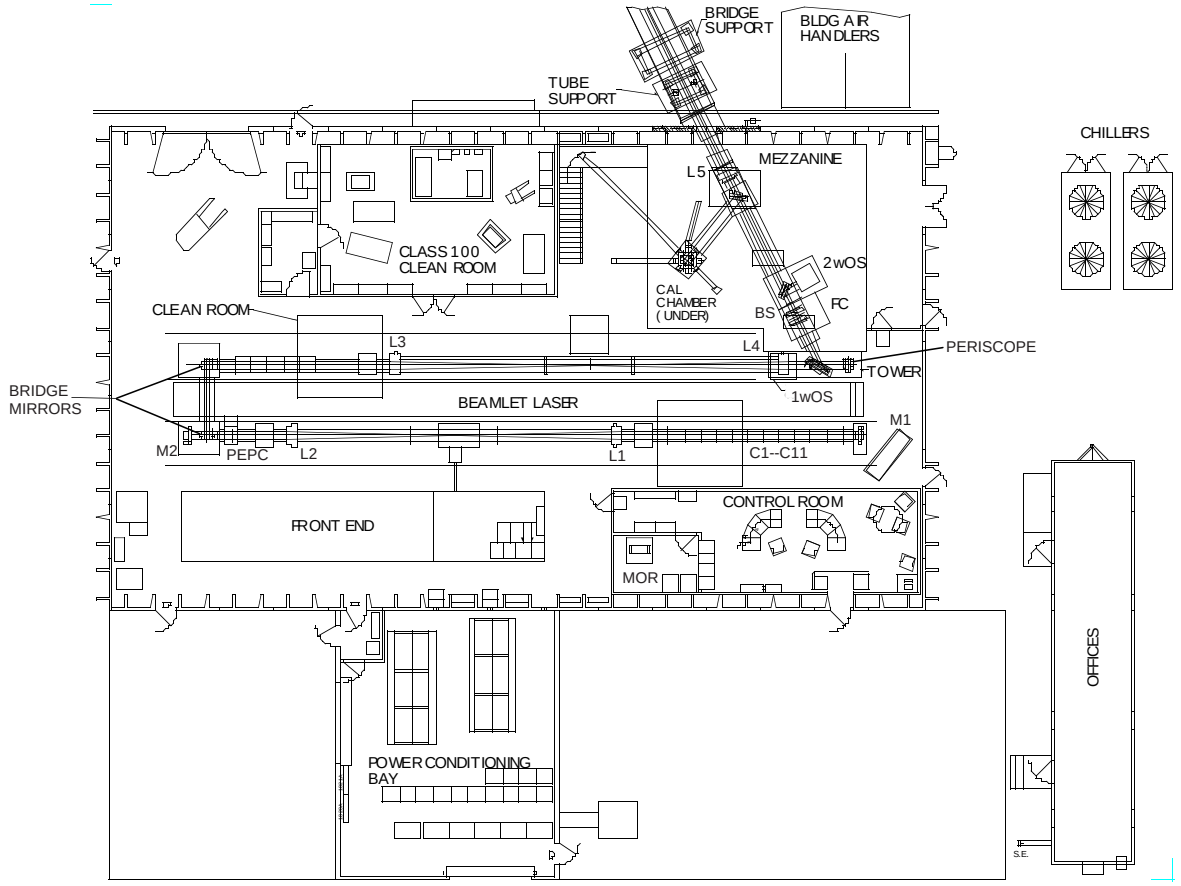

Figure 3-3. Proposed Z-backlighter architecture.

A sample of the output beam is transmitted through mirror M_8 into a new output beam diagnostic, alignment, and wavefront control system. After frequency conversion the 2ω beam is sampled by a beam splitter and diagnosed by a separate 2ω output sensor system. Alignment sensors are also provided at the focal planes of the spatial filters, and inside the target chamber as discussed in Section 3.2.4.

The layout of components shown in **Figure 3-4** was chosen to allow the input aperture to be relayed from M_1 to M_2 to M_8 and finally to M_9. This reduces spatial beam modulation at these mirrors, thereby maximizing the attainable output energy and minimizing the damage threat to the optics. The location of the 2ω relay telescope was chosen so that it does not interfere with crane access to components in the Z-accelerator Marx banks, or water transmission lines.

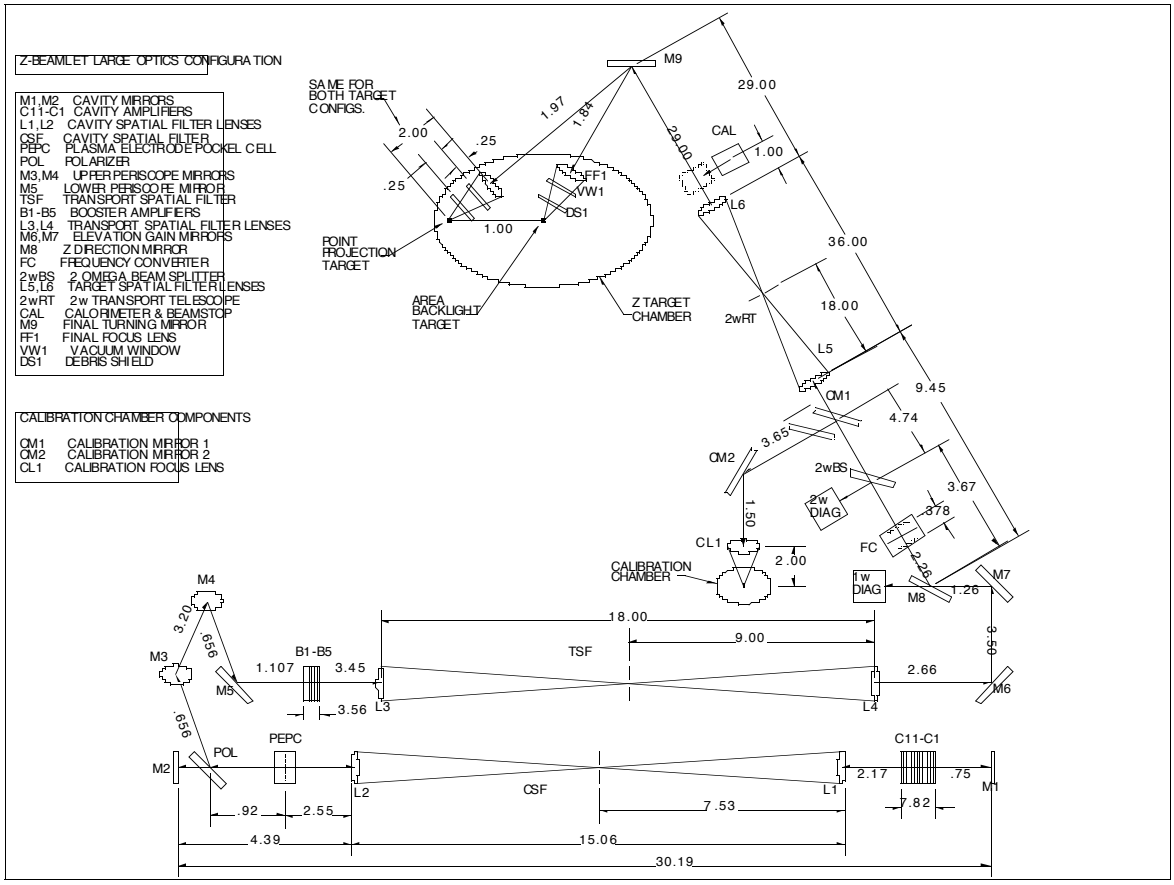

Figure 3-4. Schematic layout of the Z-backlighter laser system with component designations and dimensions noted.

Laser Performance

We modeled the performance of the laser using the PROP92 propagation code [10] in 1D with 512 grid points. This was a first-cut approach that incorporated a spatially square beam in 1D to describe the transverse beam intensity and phase profiles. Although subsequent (e.g., 2D) analyses are recommended to improve certain details, this first analysis shows that the baseline laser is robust, being capable of meeting its design requirements without any components being near their damage thresholds. In fact, the system can deliver about twice the required 3×10^{16} W/cm^2 at 2ω inside a 50-μm spot size, and about 50% more 2ω energy than required.

We based our 1ω modeling on the PROP92 input file developed for Beamlet, which includes an essentially complete front-end model. PROP92 runs with this file have accurately matched Beamlet data. We made slight alterations in some component damage thresholds to correspond to those listed below, and thickened all spatial-filter

lenses from 3.5 to 4.1 cm from the main cavity onward, but otherwise, we used the Beamlet file directly. The resultant model has an effective beam area of about 1040 cm^2.

For the 2ω PROP92 input file, we incorporated the following elements: a 2ω splitter, a relay telescope (focal length = 18 m), roughly 32 m of argon-filled transport piping, the 2ω turning mirror M9 (at a relayed position), 2.5 m of argon-filled transport piping, a 6-cm-thick final focus lens (focal length = 2 m) that served as the chamber vacuum barrier, and a 1-cm-thick BK7 debris shield. We chose the location of the debris shield to be 30 cm from the focus lens to limit its potential damage threat in the focusing beam. We considered pulse widths of 0.2 to 5.0 ns (i.e., beyond the 2.0-ns requirement) to show what performance might be achievable for extra-long pulses, in order to permit more flexible system operation.

We modeled the harmonic conversion from 1ω to 2ω with a doubler detuning angle fixed at 50 μrad (not zero) because a mounted KDP crystal typically has surface and bulk distortions that have an rms of about ±25 μrad, and absolute (not relative) alignment tolerances can be the better part of ±50 μrad. In addition, a single crystal for this laser should really be thicker than 11 mm for maximum conversion efficiency. Because we used 11 mm here, the calculated energy efficiency of the conversion to 2ω was only 72% for 0.2-ns pulse durations, dropping to 69% for 2-ns and 55% for 5-ns pulses. Optimizing the crystal thickness (or using a double-crystal configuration) could raise the conversion efficiency to at least 80%.

Table 3-1 lists the angle-independent damage thresholds that we used, in the form $F = f\tau^{\alpha}$ for threshold fluence f in J/cm^2 and pulse duration τ in ns [11]. For optics not having available 2ω damage data, we conservatively chose the 2ω thresholds to be the same as the 3ω thresholds. We assumed that damage is based on the peak intensity at an optic, and therefore assumed that the optic was damaged if any pixel in the grid exceeded the indicated damage threshold.

Table 3-1. Optical damage fluences used in the modeling.

	AR coatings	HR coatings	Laser slabs	KDP	Polarizer in trans.	Polarizer in refl.
1ω (1053 nm)	$24.6\tau^{0.40}$	$14.9\tau^{0.35}$	$22.7\tau^{0.40}$	$24.2\tau^{0.50}$	$1.3\tau^{0.50}$	$7.4\tau^{0.35}$
2ω (527 nm)	$12.3\tau^{0.40}$	$6.8\tau^{0.35}$		$7.5\tau^{0.50}$		

Table 3-2 displays the values assumed for the optical losses, and the nonlinear coefficients of the indices of refraction that formed the bases for the B-integral calculations. The loss coefficients are the effective losses at each surface due to bulk and surface losses combined, except that an extra bulk loss of 6.3×10^{-6} per centimeter was applied to all SiO_2 lenses, and a bulk loss of 0.058 per centimeter was applied to the KDP in the Pockels cell and the doubler. We assumed that all mirrors (except those actually being polarizer surfaces) had a reflectivity of 99%.

Table 3-2. Optical losses, refractive indices, and nonlinear coefficients.

Item	Debris Shield	Focus Lens	All Windows	KDP	Amp Slabs	Polarizer	S. F. Lenses
Single-surface transmission	0.995	0.995	0.995	0.995	0.9972	0.985 trans 0.980 refl.	0.995
Refractive indices	1.520 (2ω)	1.461 (2ω)	1.4498 (1ω)	1.50 (1ω)	1.519 (1ω)	1.4498 (1ω)	1ω: 1.4498 2ω: 1.461
Nonlin. coeff. (cm^2/GW)	4.2×10^{-7} (2ω)	3.3×10^{-7} (2ω)	2.7×10^{-7} (1ω)	2.7×10^{-7} (1ω)	2.9×10^{-7} (1ω)	2.7×10^{-7} (1ω)	1ω: 2.7×10^{-7} 2ω: 3.3×10^{-7}

We modeled the amplifier gain based on the actual measurements of these slabs. We incorporated optical distortions by including front and back phase-distortion maps for each optic, just as for the modeling of the NIF and Beamlet lasers. We scaled the amplitudes of these wavefront distortions to correspond to the angular orientation of each optic. These phase maps were random simulations based on the same 2D spatial frequency content as measured for Beamlet parts, including the very long (>1 cm) wavelength "phase-gradient" components. Most of these longer-wavelength distortions are removed by the adaptive optic (deformable mirror), which we included in a first-cut manner. We modeled the pump-induced distortions for the amplifier slabs based on a 1D approximation of early 2D calculations for Beamlet; the deformable mirror helps remove these effects as well. A 2D run including all distortions and an improved deformable-mirror model should eventually be made to verify the results obtained here. Both the cavity and the transport spatial filters were assumed to have pinholes set to 200-μrad half angles, but we set the 2ω relay telescope pinhole to 0.5 mrad to ease its alignment at its anticipated location.

Figure 3-5 displays the maximum 1D-performance curves for this laser. We obtained these curves by having the OPTIMA1 optimization code [12] run PROP92 by varying the input fluence (via the "outfluence" parameter) to maximize the output energy inside a 50-μm focal spot with constraints $\Delta B^* < 2$ radians, $\Sigma B^* < 4$ radians, the square-pulse-distortion ratio (i.e., the first-to-last photon-gain ratio) <35, and no pixel above the damage threshold in any optic. The B-integral constraints applied only to the beam central ray (not to a spatial average). We chose the $\Sigma B < 4$ limit because calculations showed that the peak-to-average fluence ratio at the 2ω turning mirror began to increase dramatically above this limit.

* The B-integral is the accumulated non-linear phase retardation due to high-intensity beam propagation through optical materials. ΔB is the retardation added between spatial filter pinholes, while ΣB is the total accumulation for the entire laser system.

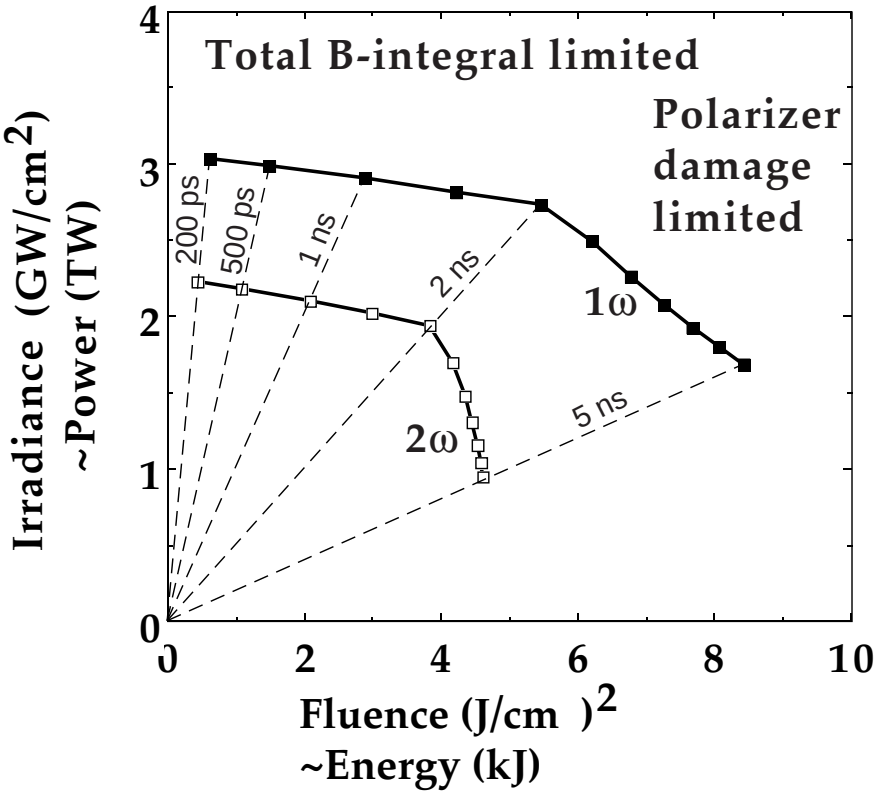

Figure 3-5. Laser maximum-performance curves. The quantities plotted correspond to the PROP92 "reference" (spatially central) ray positions at the entrance to the harmonic converter (1ω) or at the final focus lens (2ω). The dashed lines indicate 0.2, 0.5, 1, 2, and 5-ns pulse widths, respectively, proceeding from the left. The effective beam area of 1040 cm^2 can be used to convert this plot to total power and energy values.

For all pulse widths ≤ 2.0 ns, the limiting constraint was a total B-integral ≤4 radians from injection into the main-cavity spatial filter to the end of the laser chain. This total-B ignored the small contributions (each roughly 0.1 rad) from the doubler and the main-cavity transverse gain roll-off (which necessitates a larger intensity away from the central spatial ray). The maximum ΔB varied from ~1.1 to ~1.4 for pulse widths of 0.2 to 2.0 ns, and arose from the last pass (spatial-filter pinhole to pinhole) in the main cavity. Even so, a nearly equal ΔB arose in the last components of the 2ω chain after the relay-telescope pinhole. If that pinhole is set large enough to invalidate spatial filtering, then the ΔB from that section of the laser should also include passage through all components after the transport spatial-filter pinhole, and such an enhanced ΔB amounted to 2.0 ± 0.1 rad (i.e., right at the ΔB limit) for all pulse widths 0.2 to 2.0 ns. In addition, the fluences on both M5 and the polarizer increased for pulse widths greater than 0.2 ns such that for pulse widths >1.6 ns, these components were being operated above the required limit of 85% of their damage thresholds (at 2.0 ns, these components

were being operated at 91 and 98% of their damage thresholds, respectively). Thus, at 2.0 ns, there were actually three constraints in action: the total B, the ΔB, and the damage on M5 and especially the polarizer. Maximum 2ω output is 2.3 TW at 200 ps, and ~4 kJ at ≥2 ns.

Other performance parameters did not present any difficulties. The square-pulse-distortion ratio (i.e., the first-to-last photon-gain ratio) never exceeded a value of 3. The injection energy into the main cavity was always less than 0.5 J. This low input energy allows the flexibility to change the flashlamp arrays from the Beamlet configuration to a lower-gain double-sided configuration without exceeding the limits on the front end.

For pulse widths of 2.5 to 5.0 ns, the limiting factor is damage to the main-cavity polarizer on reflection. Of significance, however, is that such pulse widths cause, respectively, ~90 to 120 J to be deposited on the main-cavity spatial-filter pinhole assembly (and almost a comparable amount on the transport spatial-filter pinhole assembly). Doubler efficiency varies from 66 to 55%, but the energy delivered inside the 50-μm focus spot is 3.5 to 4.1 kJ.

Figure 3-6 shows a typical far-field focus of the 2ω beam at 2.0 ns, and **Figure 3-7** shows its line integral. Note that a focal spot diameter of 50 μm contains about 89% of the beam energy. The "spikiness" is produced by laser speckles, which are resolved in this calculation.

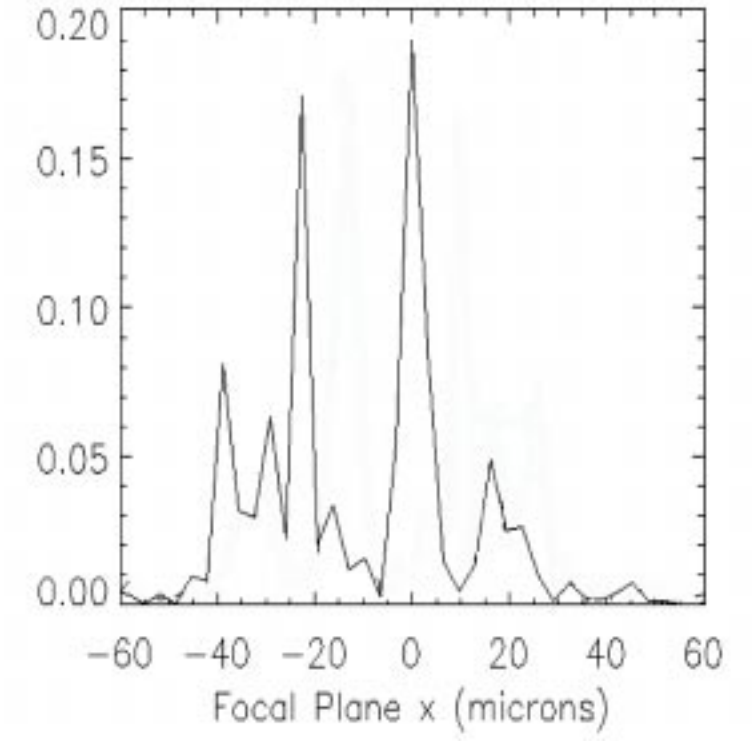

Figure 3-6. Focal-plane 2ω intensity distributions (in relative units) for 1D calculations at 2 ns with the relay telescope.

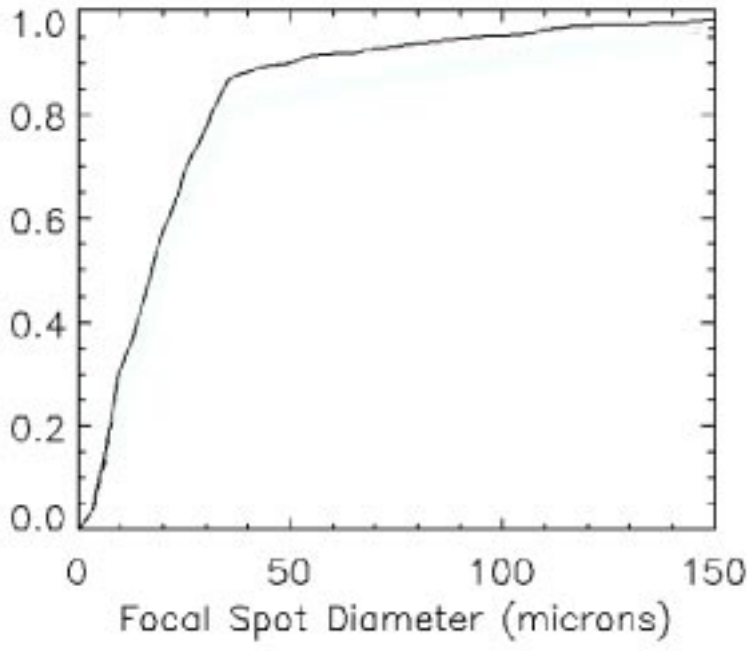

Figure 3-7. The integral from –x to +x of the curves in Figure 3-6, normalized to unity for large values of x, and plotted vs. 2x (the diameter of the region of interest).

Table 3-3 lists the fractions of the total output energies contained within a focal spot of 50-μm (square) diameter for all of the pulse durations. Note that the fractional energy within the focal spot is larger than the required 80% for all cases.

Table 3-3. Fractions of the total energy within a 50-μm focal spot.

0.2 ns	0.5 ns	1.0 ns	2.0 ns	5.0 ns
0.859	0.865	0.874	0.887	0.933

One result of interest for the spatial filter in the main cavity is that the energy dumped on the pinholes increased from about 10 J at 0.2 ns to 80 J at 2 ns. This loading of the pinholes suggests that an appropriate selection of materials will be needed for these pinholes, or larger pinholes must be considered.

Although the performance curves and other results presented here show that the laser as designed does meet its requirements, there are uncertainties in the modeling for two reasons: (1) there is incomplete information for certain components, and (2) the

modeling here is of a preliminary nature. In particular, although we included 1D approximations for the pump-induced distortions (which contain most of the effect), the latest 2D information has not been included. Moreover, only a first cut was made in the 1D calculations to optimize the input spatial and temporal profiles of the beam. An attempt should therefore be made to gather the missing information and re-address the remaining issues in greater detail. We therefore recommend that the following actions be addressed at a future time:

- Obtain a complete set of wavefront phase distortions appropriate for the individual parts employed.
- Run with a more detailed model for an adaptive optic (deformable mirror).
- Model the propagation in 2D, and optimize the input beam's spatial and temporal profiles.
- Determine the optimum thickness of the doubler crystal.

3.2.2 Laser Optics

Design and Ghost Control

The basic optical layout closely resembles the original Beamlet cavity and transport spatial filter layout. In order to use existing room in the facility, the Beamlet cavity spatial filter has been shortened from 18 meters to 15 meters. The 9 meter square lenses can be reworked to provide the new 7.5-meter lenses. These specifications (**Table 3-4**) are consistent with re-using Beamlet's amplifiers.

Table 3-4. Beamline parameters for re-using Beamlet's amplifiers.

Pinhole spacing	2 cm square array
Beam size	34 cm
Cavity length	30 m

Amplifier cavity: Figure 3-3 shows the cavity spatial filter/relay and amplifiers. Mirror M_1 and M2 are in relay planes. The spatial filter lenses are reworked Beamlet square spatial filter lenses with a revised focal length of 7.5 meters. The spatial filter provides a 1.0× magnification and sufficient space for 11 Beamlet amplifiers. In addition, the redesigned lenses ensure that ghosts from both lenses are focused in air sufficiently far from any optical surface to ensure that no damage occurs. **Table 3-5** gives ghost focal distances for each spatial filter lens, up to 3 reflections. Note that for even numbers of reflections, light comes from the pinhole; for odd numbers of reflections light comes from the air side and is collimated. The maximum energy in the beam is assumed to be either 3000 J or 15 J depending on the pass number. There are other ghosts, which involve a reflection from M1 or M2 in between reflections from the lens surfaces. They tend to be slightly farther away from the lens than the single reflection from L1 and L2 (1.61 m), are dependent on the location of the spatial filter with respect to M1 and M2 and will be further analyzed in the next phase of the project.

Note that these ghosts between L1 and M1 also double-pass the main amplifiers. If these ghosts pose a problem, both surfaces of L1 and L2 will have to be reground so that the ghosts are moved closer to the lens.

Table 3-5. Ghost focal distances for spatial filter lens.

Lens	Ghost distance from surface of lens (m)		
	1 Reflection	**2 Reflections**	**3 Reflections**
L_1, L_2	1.61	1.14	0.64
L_3, L_4	2.11	1.37	0.81
L_5, L_6 (2ω)	4.22	2.74	1.62

Unless further ghost analysis proves otherwise, we assume that lens L1 and L2 have the vacuum radius reground to provide a 7.5-m focal length. The air radius has the original curvature but the aspheric is repolished (an additional ~2.2 microns) to restore wavefront correction. The amplifiers are spaced at least 2.17 m from L1 to avoid the single reflection ghost (3000 J). The switch is also spaced at least 2.17 m from L2 to avoid the single reflection ghost (15 J). As noted above, ghost stayout zones will be determined for all other ghosts in the next design phase and may require a further redesign of L1 and L2.

Transport spatial filter (TSF): Lens L3 and L4 are the original Beamlet transport filter lenses. In Beamlet, lens L3 was tilted 3 degrees to prevent pencil beam ghosts from propagating back through the laser. No changes are anticipated. Future plans may require 5 booster amplifiers to increase the beam energy beyond 3000 J. There is sufficient space between the lenses, booster amplifiers, and mirrors to accommodate ghost foci. Since an odd number of amplifiers is required for gain uniformity, the beam undergoes a lateral walk-off. Therefore, a single unpumped booster amplifier (B1) is included in the laser chain. Then, no realignment is necessary if and when the 5 booster amplifiers are used.

2ω Relay Telescope (2ωRT): The relay from the frequency converter to the final focus lens consists of a pair of spherical equiconvex lenses (L5 and L6), with focal lengths of 18 m at 2ω, generating a relay distance of 72 m. No component should be within 5.5 m of L5 and within 3.1 m of L6 to avoid the ghosts. A 40-cm square lens with a thickness of at least 4.1 cm is sufficient to pass a 34-cm beam and with acceptably low tensile stress.

Final focus lens: The final focus lens is assumed to be a best form (nearly plano-convex) fused silica lens, with a focal length of 2.0 m. The lens serves as the vacuum barrier to minimize glass path. The primary ghost is located about one-half of the focal length in front of the lens. The double-reflection ghost is located about 1/6 of the focal length past the lens. Turning mirror M_9, the debris shield and the phase plate must be

positioned to avoid damage. A lens to debris shield spacing of at least 28 cm will prevent ghost damage, but the beam intensification due to focusing is 1.44×. Since there are internal ghost foci which will cause damage, a design strategy similar in approach to that of the Nova final focus lens will be required. The Nova lens had an annular groove machined into it to prevent internal ghosts from coming to focus.

Optical Coatings

The majority of the coated optics will come from the Beamlet and Nova laser system, but some unique requirements of the Z-Beamlet laser, such as the 2ω turning mirror, necessitates the manufacture of new optical components. Because we have never fabricated a full-aperture 2ω turning mirror, we fabricated and damage tested several 15-cm 2ω mirrors to certify compliance with the assumed damage threshold in excess of 10 J/cm2 at 3-ns pulse length.

The damage test optics were coated at Spectra-Physics, a qualified NIF coating vendor, utilizing deposition technology developed for NIF 1ω transport mirrors. The damage tests were conducted at LLNL on the Chameleon damage tester using the raster scan technique. A 80-mm × 80-mm central square was tested with a nominal beam diameter of 1mm at $1/e^2$. The optic was translated in a raster scan method with a step between pulses equivalent to the 90% IO beam diameter for uniform irradiation across the surface.

The measured damage thresholds were 19 J/cm^2 with laser conditioning and 13 J/cm^2 with partial laser conditioning. The measurement accuracy of the damage tester is ± 15%. The Advanced Conceptual Design of the Z-backlighter requires a damage threshold of 10 J/cm^2 at the final 2ω turning mirror. Based on these results, we feel that an adequate damage threshold can be achieved over the clear aperture of the 2ω turning mirror with on-line laser conditioning. The recommended laser conditioning routine is the same as past conditioning on 1ω Beamlet optics consisting of six steps of equal increment starting at one half the unconditioned damage threshold up to the peak operating fluence of the mirror.

3.2.3 Mechanical Systems

Master Oscillator Room (MOR)

The oscillator for the laser system will be a new design that is a rack-mounted solid-state system which does not require opto-mechanical supports. The only HVAC requirement for the MOR is room temperature control to ± 2.0°C.

Front End

The oscillator will feed into amplifiers that are part of the existing Beamlet front-end system. The Front-End System optics and mechanical supports from the regenerative amplifier to the 4-pass rod preamplifier will be reused from Beamlet. A clean room

enclosure will be built around the front-end similar to the enclosure that existed around the Beamlet front end.

Beam Injection

The injection of the beam from the front-end into the amplifier cavity will be done with the Beamlet injection system. The last spatial filter before injection (SF5) may need to be rebuilt with different lenses to accommodate the focal length of the Z-Beamlet cavity spatial filter and injection location change. In other respects, the Beamlet injection table, pinhole assembly, and injection enclosure will be unmodified. Vacuum pumps similar to the Beamlet system will be used to maintain the necessary low pressure in the injection enclosure and spatial filter tubes.

Cavity Spatial Filter

The Beamlet cavity spatial filter will be used with a modification to the current 9-m focal length and the front-end injection location. The 2 end sections of the 3-section transport tube will be shortened to accommodate a 7.5-m focal length. Lenses L_1 and L_2 will be ground from the Beamlet L_1 and L_2 lens. The Beamlet transport tube support towers and optical mounting hardware will be reused. A cryopump will be purchased for the cavity spatial filter vacuum system to replace the Beamlet cryopump, which was allocated to the NIF Project. A rail-mounted HEPA filter enclosure will be used as a portable clean room to access optics along the cavity spatial filter line.

Amplifiers

The Beamlet amplifiers and support rails will be used in the existing four-pass, eleven-slab configuration. The Beamlet amplifiers are configured into 4 cells that form a 2 × 2 array, which will be reconfigured to a 1 × 2 array to save on required pulsed power. Z-Beamlet will have active laser glass installed in one cell only with the remaining cell having an inexpensive architectural glass. Nitrogen gas will be supplied to the existing amplifier gas inerting system.

End Mirrors (M_1 and M_2)

The cavity spatial filter end mirrors will be the 61-cm-diameter Beamlet end mirrors. The Beamlet optical mounts and enclosure housings will be used. M_2 will be housed in the Beamlet optics enclosure with the polarizer and M_3. The enclosures will be connected to the nitrogen gas system to reduce exposure to contaminants.

Pockels Cell

The Beamlet Plasma Electrode Pockels Cell (PEPC) will be installed at the output end of the cavity spatial filter next to the polarizer. Some internal modifications to the anode will be made to make the plasma more uniform, but the bulk of the PEPC will remain unchanged. The Beamlet PEPC support structure will be used.

Polarizer

The rectangular Beamlet polarizer will be used (in conjunction with the PEPC) to switch the beam out of the cavity after the fourth amplifier pass to M_3. The existing optic, mount, and enclosure will be used for Z-Beamlet.

Turning Mirrors (M_3, M_4, and M_5)

After the beam is switched out to M_3, it passes over the bridge to M_4 and M_5, which direct the beam for a single pass through the transport spatial filter. M_3 and M_4 will be the 65.5-cm-diameter Beamlet mirrors. M_5 will be the rectangular Beamlet optic similar to the polarizer. M_4 and M_5 will be housed together in the Beamlet enclosure on the input end of the transport spatial filter. The enclosure will be connected to the nitrogen gas system.

Transport Spatial Filter

The Beamlet transport spatial filter with a 9-m focal length will be used for the Z-Beamlet system. The focus lens L_3 and L_4 with mounting hardware will be from Beamlet. All transport tube support structures will be reused. This is a vacuum spatial filter, so a cryopump will be purchased to replace the Beamlet cryopump, which was retained by the NIF Project. A rail-mounted HEPA filter enclosure will be used as a portable clean room to access optics along the transport spatial filter line.

Periscope

Mirror M_6 will direct the output beam upward to the M_7 mirror, which will be at the same height as the 2ω relay telescope delivering the beam to the Z-pinch target chamber. M_6 and M_7 will be 65.5-cm-diameter Beamlet or Nova mirrors supported with a standard mount (Aerotech) for this size optic. An additional mirror (M_8) will leak 1ω light into the 1ω diagnostics package. This mirror will be a 94-cm-diameter output sensor mirror from Nova, which will be supported with its standard mirror mount. A new space frame structure will be designed to hold these three mirrors in the proper locations. A sheet-steel enclosure, with a nitrogen purge, will cover these optics to maintain a clean atmosphere around these optics.

Laser Diagnostics

A 1ω laser diagnostics package will be designed to be located behind the M_8 mirror. This places the package directly above the end of the transport spatial filter at the same level as the 2ω relay telescope (2ωRT). The supporting space frame will need to accommodate maintenance access to these areas. The package itself will be a new design in a new enclosure, but it will resemble the existing Beamlet diagnostics package. A similar 2ω laser diagnostic package will also be located between the 2ωRT level and the frequency converter. A large-area calorimeter will be located after the output lens of the 2ωRT.

Frequency Conversion

The 1.06-μm beam generated in the main cavity is frequency doubled to 0.53 μm after leaving the 1ω laser diagnostics. Existing Beamlet crystal mounts and enclosure will support and protect the crystal. A space frame will need to attach to the same support points that the enclosure has in the Beamlet configuration.

2ω Relay Telescope

The 2ω Relay Telescope (2ωRT) transports the beam half of the distance from the laser facility to the Z-pinch. It has a 44-cm square lens at each end (fabricated from Nova lenses) and a personnel-accessible pinhole assembly at the center. High-vacuum pumps at each end will keep the internal pressure below 10^{-4} torr. A vibration-isolated external housing will traverse the space between the buildings and will protect the 2ωRT from weather and wind-induced motion. The 2ωRT will not touch the housing structurally, but is supported on space frames that penetrate the housing floor through rubber boot seals. The bridge-like housing is supported at each end by structural steel frames on separate concrete foundations. Seals at each end of the housing will keep controlled-temperature air from the laser facility moving slowly though the insulated housing to keep the temperature within ±5°F.

Transport Tube

The transport tube for the 2ωRT maintains the line-of-sight between the end of the 2ωRT and the final turning mirror located over the Z-pinch chamber. This tube will have a non-scattering controlled atmosphere of argon to keep the output face of lens L_6 free of airborne contaminants. The output end of the transport tube may have a window, or may directly attach to a beam tube around the final turning mirror. This choice depends on the design chosen to accommodate mirror mounting and the daily removal of the Z-pinch chamber lid. The turning mirror enclosure will be removed daily to permit Z-pinch chamber lid operations. The transport tube and turning mirror enclosure will be fitted with guillotine (or knife-gate) valves, manually actuated to seal the clean interiors of the tube and enclosure from the high-bay atmosphere. The transport tube can be supported with low-cost space frames, because its alignment is not critical to the laser performance.

Laser System Supports

The laser system components will be supported off the floor using carbon–steel space frames. The majority of the smaller supports will be made from 4-in. × 4-in. square tubing. The space frames will not include any precision alignment hardware, as that will be part of the optics mounting hardware supported on these frames. They must be rigid enough, however, to maintain the pointing stability of the optical elements. In most cases, the frames will be set on 2-foot-thick concrete piers individually poured on the ground, and independent of the general B986 bay floor. The

exception is the 2ωRT, which will be supported on 3-foot-thick piers with 6-inch square tube space frame supports.

2ω Turning Mirror (M_9)

The 2ω turning mirror directs the output beam from the transport tube downward towards the focus lens and the backlighter target. This mirror is designated M_9, and will be a re-coated mirror from Nova. The mirror support will need to be motorized to permit alignment to the target. In addition, to accommodate both the large area and point backlighter schemes, the mirror will need to have significant travel in its angular adjustment, on the order of 10°. Supporting this mirror above the chamber, with the necessary pointing accuracy, represents a significant engineering challenge. The support will also have to incorporate some local temperature control, as the ambient air temperature in the Z-pinch high bay is not well controlled.

Final Optics Assembly

The final optics package (see **Figure 3-8**) consists of the focus lens/vacuum window, a diffractive optics plate (for some shots), and a debris shield. All optical components will likely be located in a re-entrant tube inside the Z-pinch chamber, and will require new mounts. Since the Z-pinch chamber is a vacuum vessel, the final optics package must have a vacuum barrier, most likely the focus lens itself. The lens mount must permit at least axial motion (motorized) during alignments to the backlighter target. The debris shield is expected to be destroyed by shrapnel from the Z-pinch, so its mount must permit rapid exchange for a new shield. Because of the shock generated in the Z-pinch event, the mounts for all the optics must be designed to damp strong motion so that the optics are not shattered by the shock. Mounting techniques will be tested in a risk-reduction phase during FY99.

Target Assembly

A manipulator and feedthroughs must be designed for backlighter target insertion into the Z-pinch vacuum chamber. X-Y position adjustments will be necessary to place the target in the proper location. The structure must either be robust enough for the bulk of it to survive the shot, or the positioner must be such that it can be replaced on each shot.

Target Alignment System

A manipulator must be designed for the target alignment camera to permit its insertion into the location of the backlighter target. After alignment, the camera must be rapidly withdrawn into a protective "garage," and the target put in place with a similar manipulator (described above).

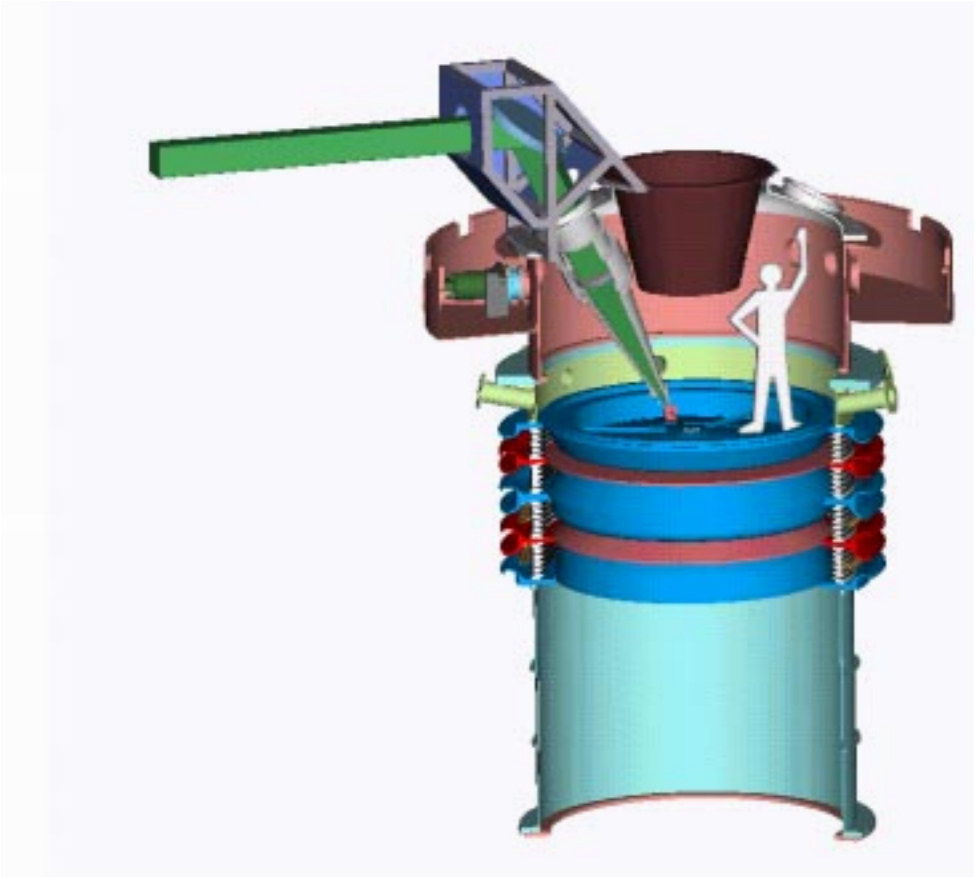

Figure 3-8. Conceptual Design of the Final Optics Assembly.

Cleaning and Assembly Workstations

A variety of equipment is required inside the 770-ft^2 clean room located in B986 to clean and process the laser optical components. An aqueous cleaning system will be used for initial cleanup of optics. A CO_2 frost system will be used to remove surface contamination. Additional cleaning work will use a deionized water workstation in the cleanroom. For work with the large optics, a number of handling devices will be needed, including fixtures for lifting or assembly, cleanroom tools, and an overhead crane system. An assortment of consumables is required for clean room work, such as coats and wipers. Finally, cleanliness measurement devices will be used to ensure that the clean room system is functioning at the required level (Class 100).

In addition to these workstations, portable cleanrooms (100–200 ft^2) will be required to cover laser sections undergoing maintenance or component replacement. This will ensure that contamination of the beamlines is kept to a minimum.

3.2.4 Laser Alignment and Diagnostics

Alignment

Beamline alignment capability implies the ability to center and point the beam at each location along the beam path where there is the potential for misalignment. There are three such segments in the Z-Beamlet layout, as shown in the schematic diagram in **Figure 3-9**. These are the segments with the cavity spatial filter (CSF), the transport spatial filter (TSF), and the 2ω relay telescope (2ωRT). Each of these requires pointing and centering capability. In addition, alignment capability for the harmonic generators and for the target must be provided.

For centering, insertable X-hairs will be used as references to mark the desired positions of the beam center. The centering procedure requires moving the beam transversely to center it on the X-hair, using a diagnostic that shows the near field of the beam down-beam from the alignment position. The shadow of an aligned X-hair inserted up-beam serves as a reference to mark the beam center. The locations of three insertable X-hairs for the Z-Beamlet layout are shown in **Figure 3-9**. X-hairs #1, #2, and #3 will be used for centering in the CSF, TSF, and 2ωRT sections, respectively.

For pointing, the references will be the spatial filter pinholes for the CSF and TSF segments, and a 1ω pointing detector in the 2ω output sensor for the 2ωRT segment. For aligning through the pinholes in the TSF and CSF, the position of the beam at the pinhole will be monitored with long-working-distance microscopes (e.g., instruments made by Questar Corp.) focused on the plane of the pinhole. Since pinholes used for system shots are hard to view, due to their inherent low scatter and reflectivity, special alignment screens will replace the pinholes during alignment. Encoded translation or rotation stages will replace alignment pinholes with shot pinholes.

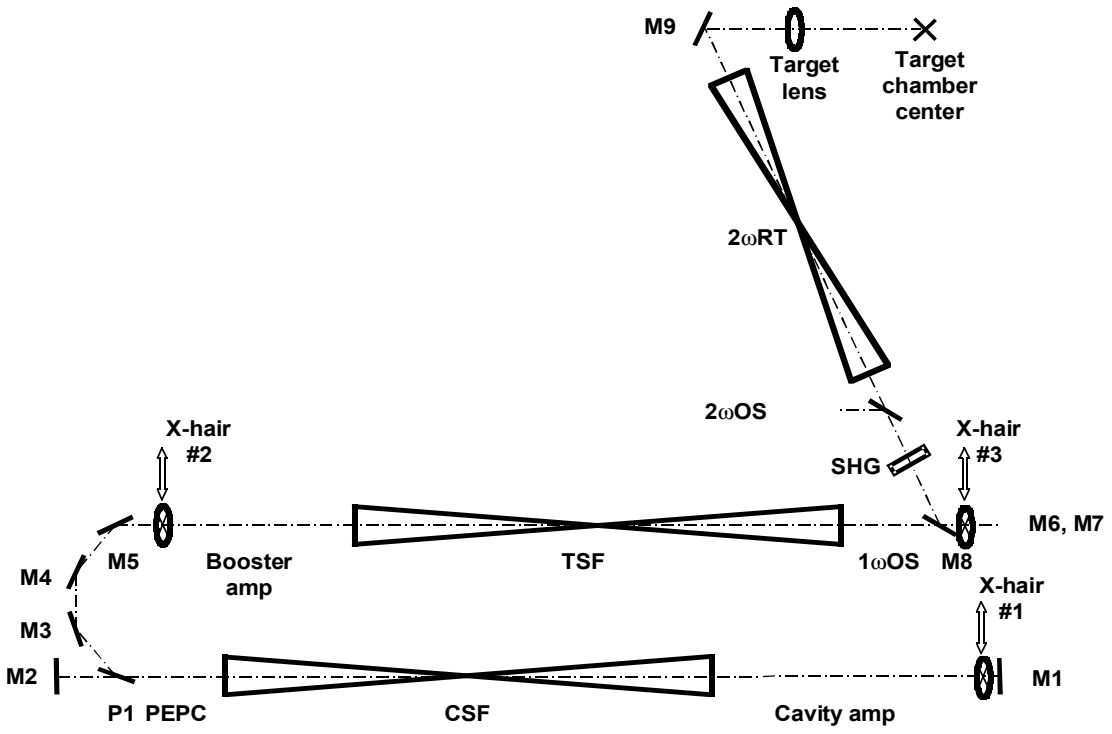

Figure 3-9. Schematic diagram of Z-Beamlet laser system with major alignment and diagnostics components.

Initial alignment of the second harmonic generator (SHG) will be done by re-configuring the front end to deliver 200-ps pulses from the regenerative amplifier system (regen). The SHG will then be aligned by maximizing the 2ω energy generated by these pulses, using a CCD viewing the focal plane at the 2ωRT. The CCD will be mounted outside the vacuum, and an insertable mirror will reflect the beam to the CCD through a vacuum window. The repetition rate of the regen, one pulse every 5 seconds, compared to one every 20 minutes for the rod amplifier pulses or one every 3 hours for the full system, allows for a reasonable time for this initial alignment.

The energy/pulse for this SHG alignment scheme can be determined from the small-signal conversion efficiency (η) for a 1.1-cm-thick KDP Type I SHG: $\eta = I_{2\omega}/I_{1\omega} = 0.5$ cm^2/GW.* Assuming 5 mJ, 200-ps pulses at the output of the regen, 8% transmission through the front end, and 25% through the full-aperture disk system to the SHG, gives 0.5 MW of 1ω at the SHG. Further assuming a 1000 cm^2 beam area gives a maximum pulse energy at 2ω (i.e., for perfect alignment) of $E_{2\omega} \sim 30$ pJ. To increase confidence in this prediction of SH energy, we did a quick measurement of the 2ω energy generated

* Private communication between Mary Norton and Jim Murray.

this way using the Beamlet full-aperture SHG and the regen. The measured 2ω energy was within a factor of 2 of the prediction.

We propose to detect this at the 2ω focus of the 2ωRT with color filters to eliminate unconverted 1ω energy. At this location, the best-focus beam size will be ~220 μm in diameter, giving a 2ω fluence (for perfect HG alignment) of ~80 nJ/cm^2. A silicon CCD, whose saturation intensity at 2ω (0.527 μm) = 80 nW/cm^2 integrates energy during the 1/30 sec framing time of the electronics, giving a saturation fluence of ~3 nJ/cm^2, or about 25 times less than the peak 2ω signal. Assuming a factor of ~100 between saturation and noise for the CCD, it will be able to detect a 2ω signal ~800 times less than the peak (with a signal-to-noise of 3). This will give a detectable signal with the KDP misaligned by as much as 0.5°. Once a 2ω signal is acquired, the output of the regen can be adjusted to prevent saturation of the CCD. The orientation of the KDP will be adjusted for maximum signal using a line-out from the video system to show the amplitude of the SH signal. The harmonic generator will be encoded to allow returning to this orientation during routine alignment, but the above procedure will always be available to check the encoded positions.

Target alignment will also use the 2ω energy generated by the regen pulses for positioning the target and focusing the lens on the target. A vacuum-compatible CCD with color filters to block the 1ω light will serve as a surrogate target and be positioned at the location of the target in the chamber. The F-number of the target lens will be substantially smaller than the 2ωSF lens (6 compared to 26), which will decrease the focused spot size to ~50 μm, increasing the fluence by $(26/6)^2$ to 1.5 μJ/cm^2 at this CCD . Consequently, the same assumptions as before (a saturation fluence for the CCD of 3 nJ/cm^2, a detectable fluence 100 times lower than the saturation fluence, and a minimum signal-to-noise of 3) give a signal 16,000 times greater than the minimum, which will give a detectable signal 3.9 mm from best focus of the target lens. Once a 2ω signal is acquired, the spot size will be minimized using the video display from the CCD. The output of the regen will be attenuated to avoid saturation and allow fine adjustment for minimum spot size. At shot time, the CCD will be moved into an armored enclosure[1] to protect it from target shrapnel and replaced by the real target, using an encoded translation stage.

Aligning the pinhole in the 2ωRT will be done using an auxiliary 2ω source[2] (a 527-nm laser) and the target-chamber CCD positioned at best focus in the target chamber. The source will be injected into the 2ωRT with appropriate optics to overfill the 2ωRT pinhole. The source will be mounted in air, outside the 2ωRT vacuum, and

1. A disposable CCD might be used in place of the current target-chamber CCD to eliminate the problem of protecting this CCD when the Z-accelerator fires. The disposable CCD would have to be vacuum compatible, approximately as sensitive as the current one, and inexpensive enough to replace after every shot.

2. A different wavelength than 2ω (532 nm) might be found for the green alignment laser that is cheaper than the doubled YLF laser envisioned, if the wavelength difference did not defocus the pinhole image at the target chamber CCD too much for pinhole alignment.

brought in through a window to an insertable mirror centered on the 2ω beam. The CCD in the target chamber will then show an image of the pinhole, which can be centered on the pre-determined position of the main-beam focus. (The power of this laser and the reflectivity of the three 1ω turning mirrors, M6, M7, and M8, will have to be specified to deliver adequate 2ω power to the target chamber for this task.)

Table 3-6 summarizes all the alignment tasks for the Z-Beamlet system. The order of alignment tasks is one that works; others will certainly be possible.

Table 3-6. Z-Beamlet system alignment tasks.

	Component	Alignment function	Alignment reference	Detector	Illumination source
1	CSF segment	pointing	CSF pinholes	Questar #1 @ CSF	fiber-optic source @ CSF pinhole
2	"	centering	Insertable X-hair #1	nf detector in 1ωOS	1ω alignment laser
3	TSF segment	pointing	TSF pinhole	Questar #2 @ TSF)	fiber-optic source @ TSF pinhole
4	"	centering	Insertable X-hair #2	nf detector in 1ωOS	1ω alignment laser
5	2ωRT segment	pointing	pre-determined spot on CCD	1ω ff detector in 2ωOS	1ω alignment laser
6	"	centering	Insertable X-hair #3	nf detector in 1ωOS	1ω alignment laser
7	SHG	orientation	Max SH signal from regen	CCD @ 2ω focus in 2ωRT	MOR and front-end regen
8	Target	focusing & positioning	position & min size of focus	CCD @ best focus in TC	SH from regen and SHG
9	2ωRT pinhole	positioning	pre-determined spot on CCD	CCD @ best focus in TC	2ω laser injected @ TSF

Diagnostics

Diagnostics are used to perform two types of functions: (1) alignment of the system prior to a shot; and (2) diagnosing the pulsed beam at various points in the system during a shot. Several diagnostics are used in both capacities and therefore require variable neutral density (ND) filters to accommodate the range in intensity between the continuous wave (CW) alignment beam and the pulsed beam. The front-end system will use the diagnostics systems from Beamlet with relatively little modification. For the full-aperture beam, most of the alignment diagnostics were described above. Those that were not are in the 1ω or 2ω output sensors (1ω OS and 2ω OS, respectively).

Schematic diagrams showing the functionality of the two new output sensors are shown in **Figures 3-10 and 3-11**.

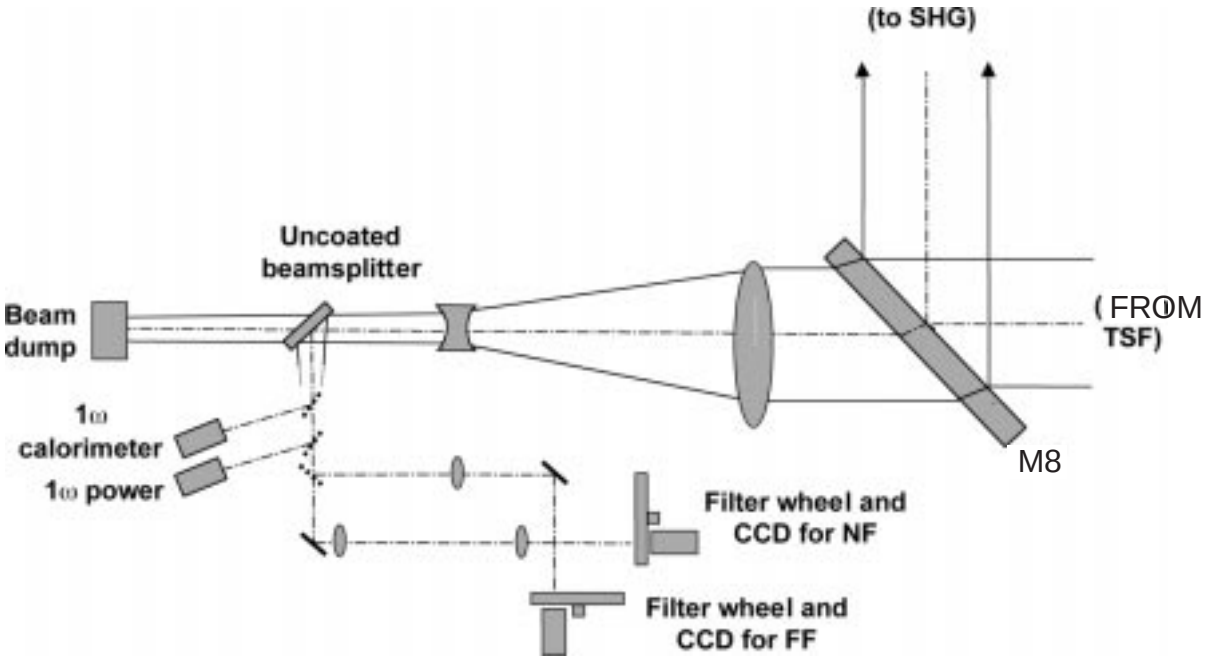

Figure 3-10. Schematic of a 1ω output sensor.

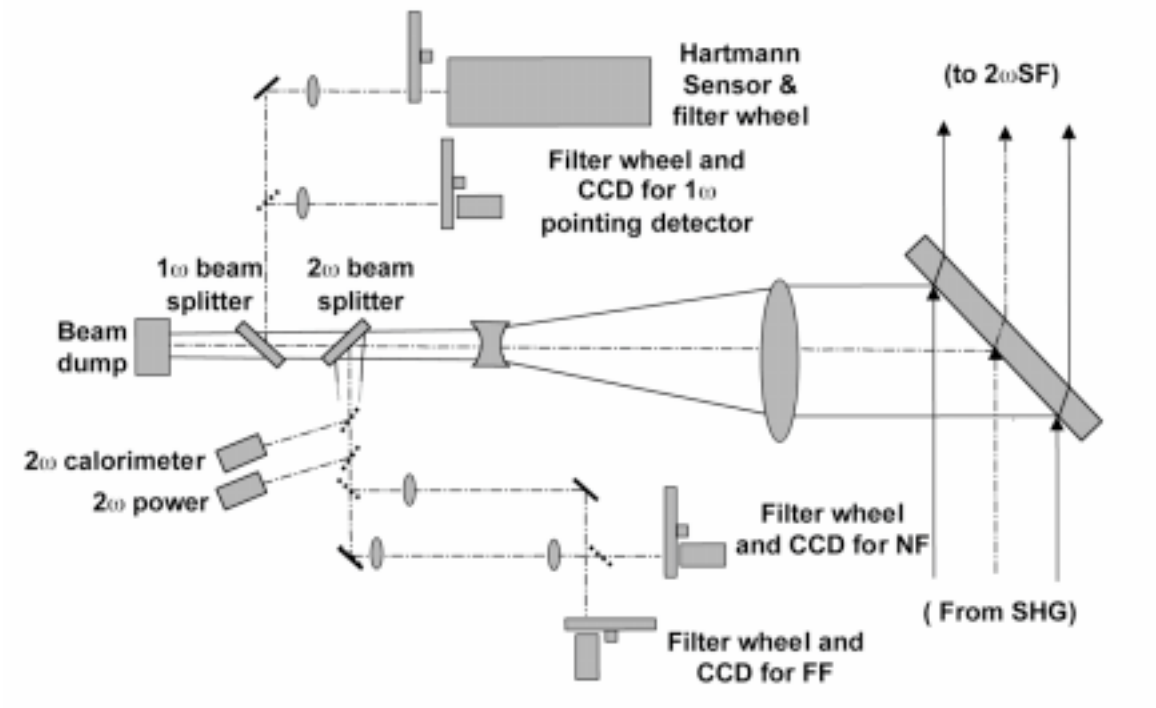

Figure 3-11. Schematic of a 2ω output sensor.

The 1ω OS performs four diagnostic functions during shot mode and three during alignment, by sampling the beam directly out of the cavity. During shot mode it provides measurements of near field, far field, energy, and power of the 1ω output beam. During alignment it provides a view of the 1ω near field to center the beam at X-hairs #1, #2, and #3.

The 2ω OS also performs four diagnostic functions during shot mode but only two during alignment. During shot mode it provides measurements of near field, far field, energy and power of the 2ω output beam. During alignment it provides a view of the 1ω far field that serves as a pointing detector, and it provides a 1ω near-field view to the Hartman sensor for wavefront control. (Note that the instrumentation for reading out all the fast diodes simultaneously may not always be available.)

An insertable, full-aperture calorimeter at the output of the 2ωRT provides a means of calibrating the energy monitors in the 1ωOS and 2ωOS. With the SHG misaligned and the pinhole out of the 2ωRT, the calorimeter reads the 1ω output energy of the system; with the SHG aligned and the pinhole in the 2ωRT, it reads the 2ω output energy. The insertable calorimeter also provides a means of isolating the laser system from the Z-accelerator, so that the two systems can be operated entirely independently.

Wavefront control

The wavefront control system corrects for optical phase or wavefront aberrations along the laser beam path. It consists of five subsystems: (1) the adaptive optic, (2) the wavefront sensor, (3) the wavefront control computer system, (4) the wavefront reference, and (5) the "T-1" system.

A glass deformable mirror (DM) has been demonstrated as an effective adaptive optic on Beamlet and other laser systems and is proposed as the wavefront correction device for the Z-backlighter. The DM contains actuators that, under computer control, deform the mirror surface in a manner to correct the unwanted aberrations.

The wavefront sensor is used to measure the local phase gradient (tilt) in the region of the beam associated with each DM actuator. A miniature Hartmann sensor has been shown on Beamlet to be an accurate yet inexpensive wavefront sensor. It consists of an array of lenslets (miniature lenses formed from a monolithic substrate) and a CCD camera to view the demagnified laser beam. The local tilt of the region of the beam associated with each lenslet is measured by the change in position of the corresponding lenslet focal spot. Tilt measurements from the lenslet array representing the entire beam aperture are then used to calculate the deformable mirror surface deformations required.

The wavefront computer control system analyzes the focal spot pattern from the Hartmann sensor, calculates the measured wavefront, and calculates the DM actuator settings to correct the wavefront in closed loop prior to the shot.

After the shot, it acquires the shot wavefront image from the Hartmann sensor and calculates the shot wavefront. It also implements online calibration routines to generate the reference wavefront and the gain matrix that relates sensor inputs to DM actuator commands to achieve a desired wavefront.

The wavefront reference is used to enable an online calibration of the wavefront sensor. The wavefront reference source proposed for the Z-backlighter is an illuminated single-mode optical fiber placed (prior to a shot) in the focus of the transport spatial filter (TSF). The reference source is viewed by the Hartmann sensor from a beam sample taken downstream of the TSF. Since the fiber core diameter is small with respect to the TSF diffraction-limited beam focal spot, the reference light wavefront viewed by the Hartmann sensor represents the way the beam wavefront would look if the laser was aberration-free up to the TSF focus. Any wavefront imperfections seen by the Hartmann sensor viewing the reference represent those associated with the sensor and its associated beam sampling and relaying optics. Thus, by controlling the DM to achieve a Hartmann spot pattern for the beam to match that of the reference, the system is, within its correction resolution limit, trying to achieve a diffraction limited beam spot at the TSF focus. It is assumed that the aberrations that occur beyond the TSF are relatively small, as the major aberrators are optic figure errors and thermal effects, and there are relatively few optics and no heat sources beyond the TSF. A good focal spot at the TSF is expected to be accurately relayed to the target.

Detailed analyses of the expected aberrations in the backlighter laser have not been conducted. However, from Beamlet experience, it has been shown that a 39-actuator deformable mirror (and associated wavefront sensor and controller) can achieve the desired beam divergence and spot size. Beamlet employs a 77-lenslet Hartmann wavefront sensor with lenslets that are mapped to half of the deformable mirror actuator spacing. Beamlet also has a fiber pick-off of its alignment laser, which may be suitable for use as a wavefront reference. A NIF-design fiber inserter will be sufficient for inserting the reference at the TSF focus.

3.2.5 Pulsed-Power Conditioning

The power conditioning electronics for the Z-Beamlet laser will be reassembled almost exactly as it was removed from Beamlet. Fewer pulsed-power components will be required because only one side of the laser amplifiers arrays will be operated. The flashlamp operating voltage will remain at a maximum voltage of 22 kV. The normal operating voltage for the flashlamps in the amplifiers has been 20 kV. The total energy storage at 20 kV will equal to 43 kJ per circuit or 430 kJ per amplifier. Total bank energy storage at 20 kV equals 4730 KJ.

The laser design consists of 11 main amplifier modules with their associated power conditioning components. The power conditioning components will be located in a

room adjacent to the laser bay. Power transmission between the power conditioning room and the laser amplifiers will use RG-217 coaxial cable routed through the wall and under the floor and terminated into the existing Beamlet junction boxes. The flashlamp wires will connect from the junction boxes to the amplifiers. Communication between the control computer and the power conditioning front-end processors will use fiber-optic network hardware.

The power conditioning system will provide energy to the flashlamps on the active side of the Beamlet laser amplifiers. The inactive side of the amplifiers will not be used. The outside flashlamp cassette from the inactive sides of the amplifiers will be fully populated with flashlamps and relocated to the center cassette holder. This configuration will illuminate the laser slabs on the active side with all 20 flashlamps. Two flashlamps are connected in series for a total of 10 circuits per amplifier.

The total circuit count for the main laser amplifiers will equal 110 circuits. Each circuit or Pulse Forming Network (PFN) will consist of a capacitor, inductor, fuse, shorting switch, and charge resistor. The PFNs will be charged using Maxwell 8000J CCDS power supply with a charge time of about 54 seconds for 0 V to 20 KV. The circuits will be discharged in parallel by a common ignitron switch assembly. The Pre Ionization Lamp Check circuitry (PILC) will be configured and operated as it has been in Beamlet. No changes to the individual PFNs will be needed from the original Beamlet design.

The configuration of the charging supply and ignitron switch circuits will not be changed from the Beamlet design. The 110 circuits will be divided between 14 ignitron switches and 14 charging supplies. Each charging supply will supply power to 8 flashlamp circuits. Input power to the charging supplies is 208V 3-phase @ 50A/phase.

The Beamlet front-end rod amplifier power conditioning equipment will be the existing design, with ~50KJ of stored energy. Input power for the rod amplifier is 3-phase 208V @ 20 A. The front-end Faraday rotator will also be the existing Beamlet design, with ~21 KJ of stored energy. The total front-end (rod amplifier and Faraday rotator) power conditioning is packaged in a space about 5 ft. square by 6 ft. high. This could be repackaged into a different size if needed. Provisions will be made for the front-end power conditioning system to charge and fire while the main capacitor bank is under construction or being maintained.

Grounding will be a single point ground at the Maxwell power supplies. All capacitor racks will be electrically insulated from the building structure and soft grounded through a resistor. All wire ways between the capacitor bank and the laser amplifiers will be non-metallic.

3.2.6 Controls System

Introduction

This system description introduces the Z-Beamlet Control System (ZCS). The design is a streamlined version of the Beamlet Computer Control System. The ZCS controls the setup and firing of the laser system used to backlight targets for the Z-accelerator, and will be a subsystem to the existing Z-accelerator Control/Monitor System (or Z C/MS). The firing of the laser is initiated by the Z C/MS.

Control System Architecture

The Z C/MS is a layered architecture consisting of front-end processors (FEPs) coordinated by their respective supervisory system (see **Figure 3-12**). Supervisory controls, which are hosted on UNIX and NT workstations, provide centralized operator controls and status, data archiving, and integration services.

There are five supervisory applications: (1) Pulsed Power; (2) Diagnostics; (3) Motion; (4) Vision; and (5) Shot Control. These functions work in collaboration with front-end processors and each other to perform various task associated with the operation of the Z-Beamlet.

Each section briefly describes the domain of the supervisor and then briefly describes its role in that domain, often with an emphasis on conducting a shot. Often tasks will require the use of several systems. For example, the alignment task requires use of the Motion, Deformable Mirror, and Vision systems. Those items with dashed outlines do not currently exist and represent a new software development effort.

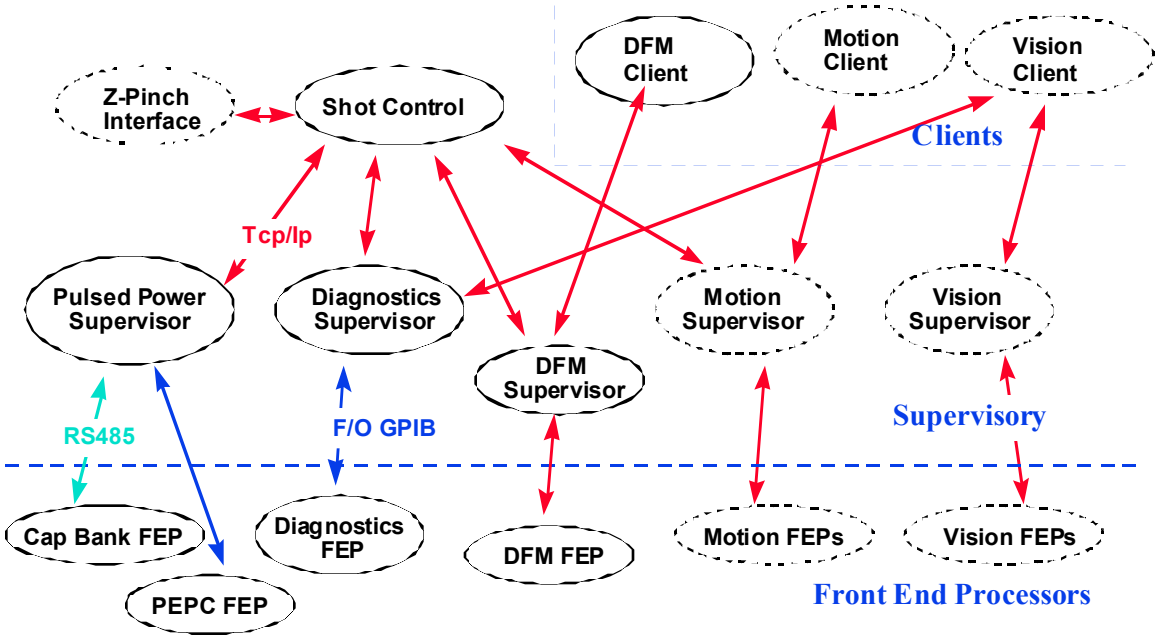

Figure 3-12. Software applications in the Z-Beamlet Control System

Pulsed Power

The Pulsed Power Supervisory (PPS) software is responsible for high-level control and management of the Plasma Electrode Pockels Cell (PEPC) and firing the main laser amplifier. Hundreds of high-voltage capacitors, along with their circuitry, are grouped into modules that are used to feed flashlamps in the main laser amplifiers. Information about the controllable devices contained in these modules must be maintained. In addition, the ability to manually control the devices for testing purposes must be provided.

The PPS performs its functions by coordinating the activities of Power Conditioning front-end processors (FEPs) and the PEPC FEP. The PPS also provides graphical user interfaces for the power-conditioning operator. To perform a shot, the PPS provides voltage settings for each participating capacitor bank. Once the shot parameters have been established, the PPS is ready to be in a shot sequence.

During a shot sequence, the PPS instructs the PEPC devices to begin their cycle. When the PEPC devices are operating correctly, a message is sent to Shot Control allowing the next step in the firing sequence. The PPS continues monitoring the PEPC operation and alerts the Shot Control of any anomalies that may occur. The PPS is allowed to begin charging the capacitor banks. The status is monitored and displayed on the PPS console. Should an anomaly be detected, either by the FEPs or the PPS Operator, the PPS will request an abort. The Shot Control will acknowledge the abort and notify the remaining subsystems that the shot has been aborted. At this point, the PPS also instructs the PEPC to start the shutdown sequence. Post shot, the PPS will

generate a report indicating the performance of the pulsed-power system and archive PEPC performance data.

Between shots, operators can use the PPS to perform a pre-ionization lamp check (PILC) to check the amplifier flashlamps. They may also use it to maintain device parameters or manually control power-conditioning devices. The PEPC system may also be run for testing and maintenance purposes.

Diagnostics

The purpose of the Diagnostics system is to control/configure the diagnostics instrumentation; acquire data and write raw data to file; summarize and display performance information to help diagnose anomalies and predict/detect potential damage to both active and passive optical components in the beam. This system collects energy, power, and image information from hardware sensors positioned strategically throughout the beam line. The diagnostic sensor list will include 5 calorimeters, 2 energy sensors (diode), 3 power diodes, 11 images, and a crystal-temperature measurement. These are distributed among 3 locations in the Z-Beamlet high bay.

Motion

The Motion Control Supervisory software provides coordination of motor and binary components. In addition, the supervisory system provides graphical user interfaces for the FEPs, maintains motion device parameters, and displays status of control points.

The Motion FEPs are Windows NT machines interfaced to a VME crate (MXI-2). The VME crate is populated by an Oregon Micro Systems Stepper motor controller. The crate also contains Themis Digital I/O cards for binary control and monitoring.

The primary activity of the motion control system is beam alignment. Alignment is accomplished by pointing and centering the beam through the laser components and pointing and focusing the laser beam on the target. This is a manual operation performed by an operator. The scope of the alignment process encompasses 29 binary and 54 motor control elements.

Vision

The Vision Supervisory coordinates the image acquisition and distribution throughout the Z-Beamlet Control area. There are approximately 21 image sources. The supervisory regulates camera configuration limiting changes during the shot sequence. The Vision Supervisory also arbitrates conflicts in image requests and terminates inactive clients to preserve the distribution system bandwidth, thereby enhancing performance. The Vision FEPs are Windows NT machines using PCI frame grabbers to acquire images on command from the Vision Supervisor or hardware trigger. At the request of the client, the acquired image can be decremented to reduced

resolution and/or zoomed to decrease the area of interest before the image is transmitted to the client via the Ethernet. Both of these processes reduce the required bandwidth imposed on the Ethernet system. Performance information is covered in the Hardware Infrastructure section below. Diagnostic images are usually complete and unprocessed.

Shot Control

The Shot Control Supervisor's responsibilities are shot formulation, shot coordination, distribution of status updates, and processing of abort requests. The Shot Control can deselect subsystems not required for a particular shot. This allows the needed flexibility to do various shot configurations for testing and maintenance. The Shot Control is the C/M interface between the Z-accelerator and the Z-Beamlet. **Figure 3-13** illustrates the shot sequence.

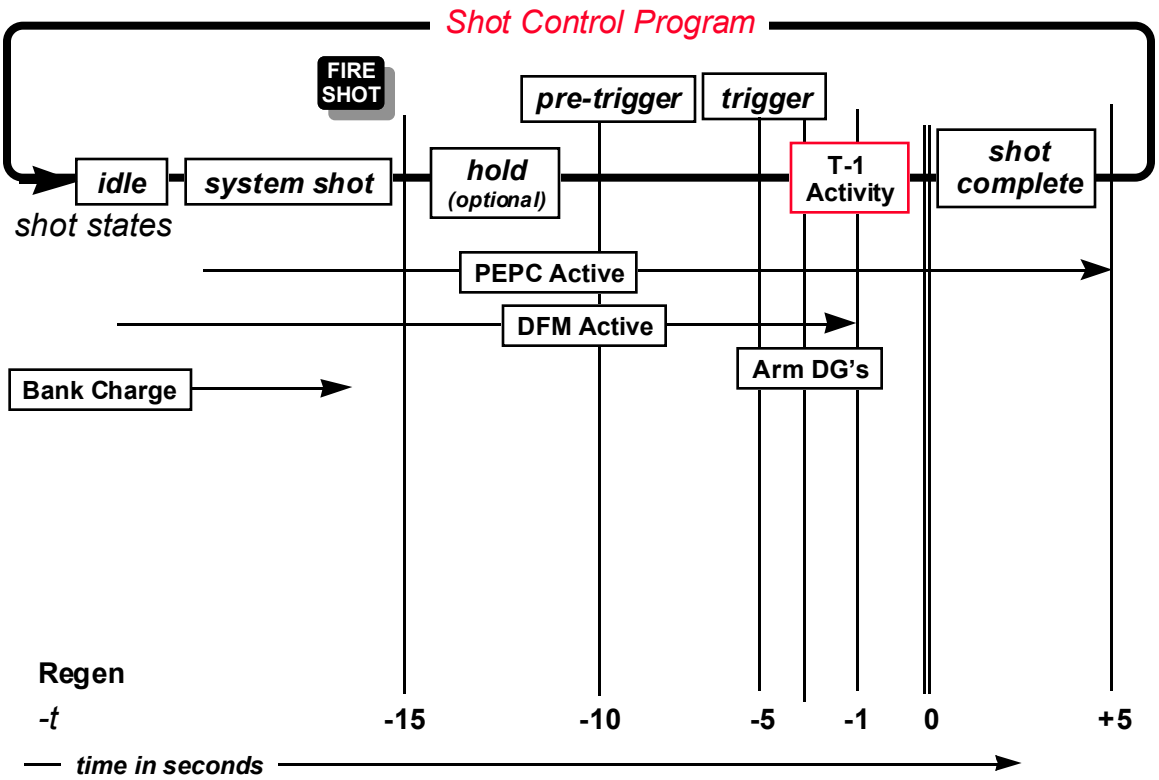

Figure 3-13. Shot Control Firing Sequence Time Line.

Hardware Infrastructure

Figure 3-14 shows the ZCCS computer system and network, which comprises several processors distributed between the laser bay and the Z-accelerator control room. The control room contains operator consoles. The applications discussed above are assigned to execute and be operated from the operator's console. Remote operation is possible from terminals located near the front-end equipment. The Diagnostic

workstation ("beamlet-srv") is the file server and the boot computer for the other UNIX computers in the system. Those items with dashed outlines do not exist and represent a procurement.

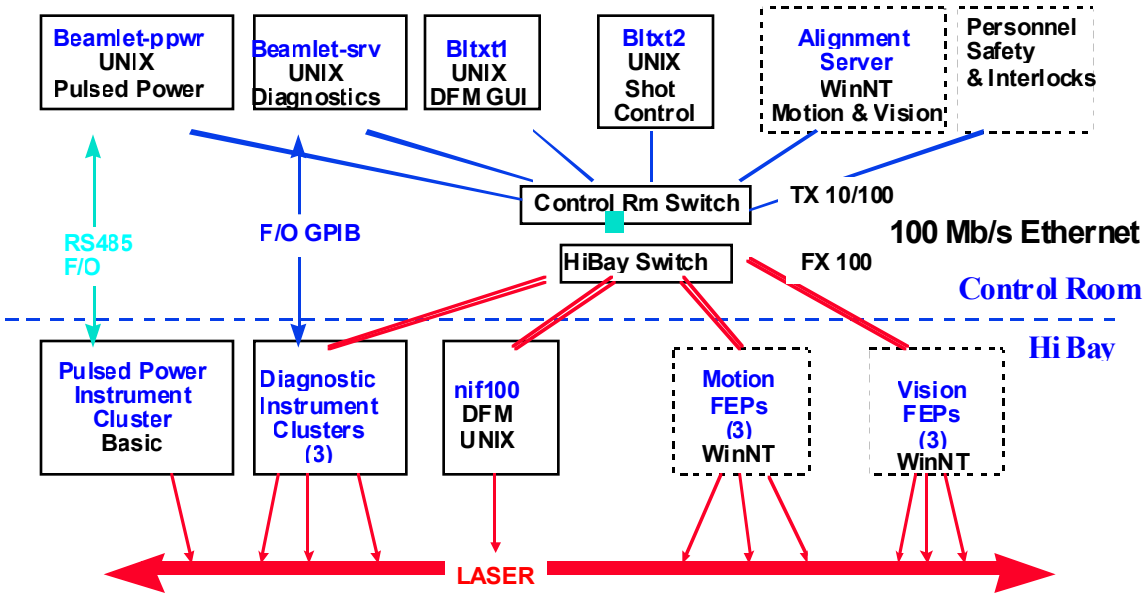

Figure 3-14. ZCCS computer system and network architecture.

Ethernet System

The network backbone is built from Ethernet switches that connect supervisory computers to the FEPs. The Ethernet System is centered on two switched hubs. The first, the Control Room Switch (CRS), is a 10/100 Mb/s switch with auto sensing to allow a seamless interface with the older equipment. The chassis will accommodate the control room and Master Oscillator Room equipment. The second chassis is called the High-Bay Switch (HBS). The HBS is an 8-port 100 Mb/s Fiber Switch that will couple to the various FEPs and instrument clusters in the high bay. The high bay hardware will use Fiber Optic Network Interface Cards (NIC) of a PCI form factor. They will provide both a high-bandwidth capability and EMI immunity. Both of these switches are coupled via a 4Gb/s back plane.

The Vision System presents the largest load on the Ethernet system. A single standard image derived from the RS170 frame capture transmitted at 10 Hz to a Vision client requires 25 Mb/s. The functional limit of the network is 33Mb/s per switched segment. This bottleneck is alleviated somewhat by the switched technology employed. The full bandwidth is preserved on portions of the network not requiring the image traffic. However, image transfers will slow on those sections of the system when more than 1 image is streamed to or from an individual segment of the network. As

previously mentioned in the Vision section, image processing prior to transmission will also increase performance.

Timing System

The Timing System is tasked with providing several sets of synchronous pulses to various subsystems. The Master Oscillator room requires 180Hz. The Vision system requires 10Hz. The Front End needs a 0.2-Hz rate for the regenerative amplifier (also called "the regen"), while in shot sequence a single pulse is required to trigger the Pulsed Power System and many of the diagnostics instruments. **Figure 3-15** displays in schematic form the proposed layout of the Z-Beamlet Timing Back Bone.

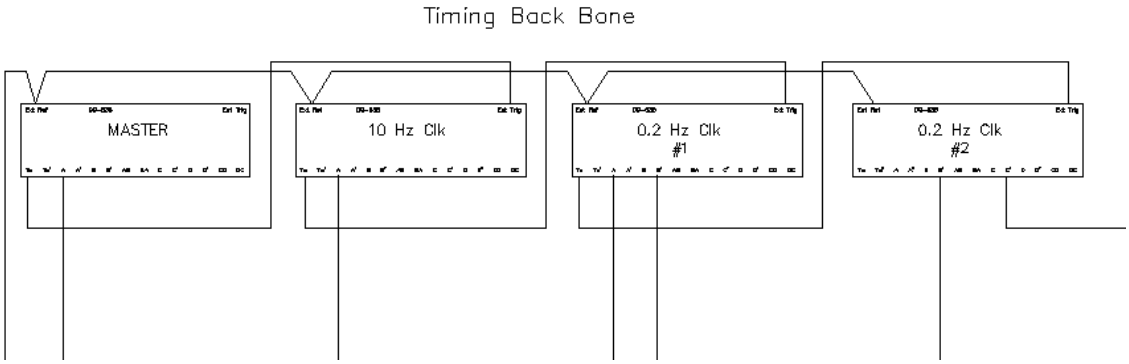

Figure 3-15. Timing System back bone.

Although it is modeled after the Beamlet Timing system, it has many of the extraneous elements removed, thus reducing the parts count and presenting a clearer system. The first chassis is the "Master." This unit sets the rate for the MOR. The second unit provides the 10-Hz clock to the Vision System. The third and fourth units generate the synchronous 0.2-Hz signal, also referred to as the "Heart Beat." The heart beat provides timing information to the front-end, PEPC, Pulse Power, and Diagnostics systems. This "heart beat" is also monitored by Shot Control to synchronize the arming of the subsystems during the final seconds of the shot sequence.

Sensors and Controls Design Direction

This *Advanced Conceptual Design Report* includes changes over the original Beamlet Control System intended to increase the reliability and maintainability of the controls system while reducing cost. Many of these changes were required due to equipment shortages realized after the Beamlet shut down.

These changes include:

- Implementation of a motor control system using a LabView-compliant platform to standardize the software development environment with cross-platform compatibility. The controls would then be 100% LabView, leading to increased ease of maintenance and less down time.
- Rewrite of the software subsystems to conform to a straightforward programming scheme, and eliminating features that contributed to erratic and unreliable behavior.
- Where needed, the use of modular instrumentation, predominantly for image acquisition, but may be expanded for other uses such as instrumentation, motor control, and communication.
- Utilization of the latest information-transfer technologies. Specifically, use of higher bandwidth (100BaseT) Ethernet for C/M and Image distribution.

3.2.7 Frequency Conversion

Overview

The 1.05 μm (1ω) wavelength of the laser amplifier will be converted to 0.527 μm (2ω) in the frequency converter assembly located in the laser bay. The baseline design for the converter utilizes type I harmonic generation in a single KDP crystal previously used on Beamlet, having nominal dimensions of 37 cm × 37 cm by 1.1-cm thick. By making use of existing crystals we anticipate achieving high conversion efficiency while minimizing the cost (this will be discussed in more detail). We also propose alternate converter designs that would improve performance but which have the drawbacks of cost or complexity.

In the baseline design, the single converter crystal will be mounted in a 24-in gimbal mount that provides pitch, roll, and yaw control. Microradian-precision tip and tilt is achieved about the horizontal and vertical axes. The crystal is held by its four corners in a diamond-turned mounting ring. The mounted crystal is located within an environmentally controlled housing. This is necessary since the KDP crystal is sensitive to moisture. Its operation at high power requires precise control of temperature and particulates. Temperature will be maintained to within ±0.6°C. Relative humidity is held to less than 35%. Particulate count is kept to better than Class 100.

Converter Baseline Design

The 1ω beam from the laser amplifier will be directed to the frequency converter crystal, termed "doubler," where it is converted to the second harmonic frequency 2ω via degenerate sum-frequency mixing as shown schematically in **Figure 3-16**. The desired second harmonic field exits the crystal along with the fraction of the input beam that remains unconverted. Energy lost in the process include the absorbed fundamental input (about 5% of the incoming irradiation), the fundamental energy reflected from the first and second surfaces, and the second harmonic energy reflected from the second surface. The polarization of the fundamental field in the crystal is directed along the crystal ordinary axis (horizontal). The output 2ω field is an extraordinary wave and will be polarized in the vertical direction.

The KDP doubler material has a bulk absorption coefficient for the fundamental wavelength propagating as an ordinary wave of 0.058/cm. The surfaces will be antireflection coated with SiO_2 sol-gel. The current coating on the Beamlet crystal is not optimized for doubler performance; instead there is a "compromise" coating on both the input and output surfaces, designed for minimum reflectance at 700 nm, which approximately equalizes the reflection losses for both wavelengths. In practice, a typical reflection loss from both surfaces is 1.8% for 1ω and 1% for 2ω. A path towards improved performance would include a re-coating of the crystal (and possibly a rework of the surface). A coating optimized for 1ω on the input surface would result in about 0.15% loss of the input energy. The output surface would be coated for 2ω resulting in only about a 0.15% loss of the converted light.

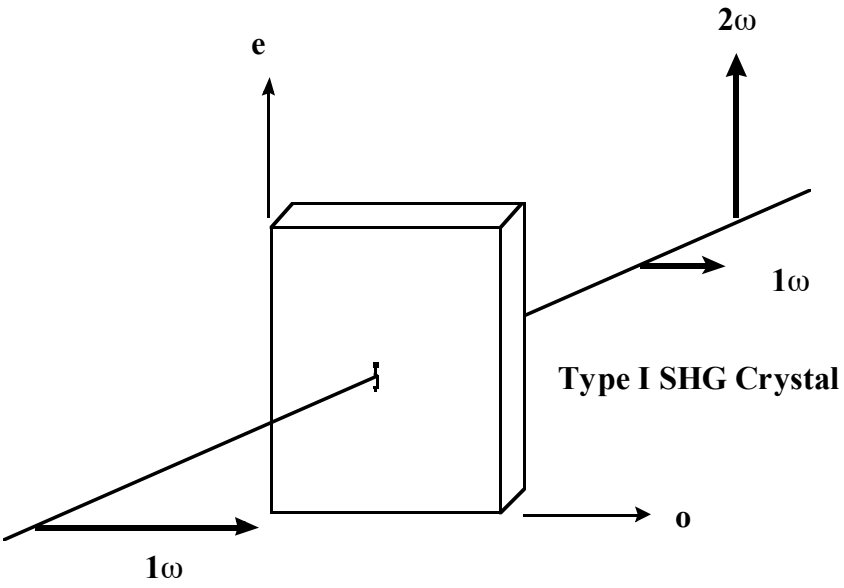

Figure 3-16. Schematic of Type I frequency conversion.

The expected conversion efficiency for the Beamlet crystals has been calculated with a plane wave model and is shown in **Figure 3-17a**. The model includes the fundamental wavelength absorption loss and nominal coating losses. The curves are parameterized by the internal angular displacement from the phase-matched condition. Better than 50% conversion is predicted for irradiance levels between 2 and 6 GW/cm^2 for a flat in space and time pulse as long as the alignment to perfect phase matched conditions is kept within 150 μrad. The anticipated working range for 0.2 to 2 ns is shown on the plot and over this operating range the conversion efficiency is expected to be better than 65%. Because the temperature sensitivity of the phase matching direction of this crystal may be as large as 118 μrad/°C, excursions in the crystal temperature of up to ±0.6°C should result in less than a 4% drop in conversion efficiency over the working range. The calculated angular tuning curve at 4 GW/cm^2 for a crystal of length 1.1 cm can be seen in **Figure 3-17b**. This curve represents the worst case as we expect to be operating closer to 3 GW/cm^2 and as can be seen in the figure there will be slightly less sensitivity

to angle 3 GW/cm^2. To keep the conversion efficiency to within 95% of the maximum achievable, the crystal must be kept within ±160 μrad of the phase-matched direction. The details of the crystal alignment process, including required beam dumps for the surface reflections, will be addressed in the detailed design phase.

Advanced Converter Designs

Because the Beamlet KDP doubling crystals were designed for efficient frequency tripling, their performance was not optimized for doubling. Therefore, it is of interest to look at what performance might be attained by utilizing two Beamlet crystals in an alternating-z configuration. The calculated plane wave performance for two Beamlet crystals utilized in this configuration is shown in **Figure 3-18a**. Here the total crystal length is 2.2 cm. If alignment is maintained to ±100 μrad, this configuration can improve the irradiance dynamic range over which high conversion efficiency is maintained. Greater than 70% conversion over a range from 0.8 to 3.4 GW/cm^2 is predicted. This design can better tolerate angular offsets and will give better performance for real beams with edge roll off and temporal Gaussian shapes because of the greater dynamic range than is possible with a single crystal design. The two-crystal design has more intrinsic loss due to imperfect coatings and requires alignment of two crystals.

If one allows for refabricating the existing crystals to a new thickness, then even better performance can be anticipated. The calculated performance for an alternating-z configuration where both crystals are reduced to 9 mm in length is shown in **Figure 3-18b**. For this configuration better than 80% conversion is predicted over the input range of 1.8 to 4.6 GW/cm^2. Thus over the anticipated working range the predicted performance is greatly improved.

One additional design considered is a single crystal, thicker than the existing crystals. For instance, the performance of a 1.4-cm-thick crystal is shown in **Figure 3-18c**. Again this shows better performance over the intended working range. Further work would be required to optimize a single crystal design to balance the gain in higher efficiency against the increased sensitivity to angular misalignment.

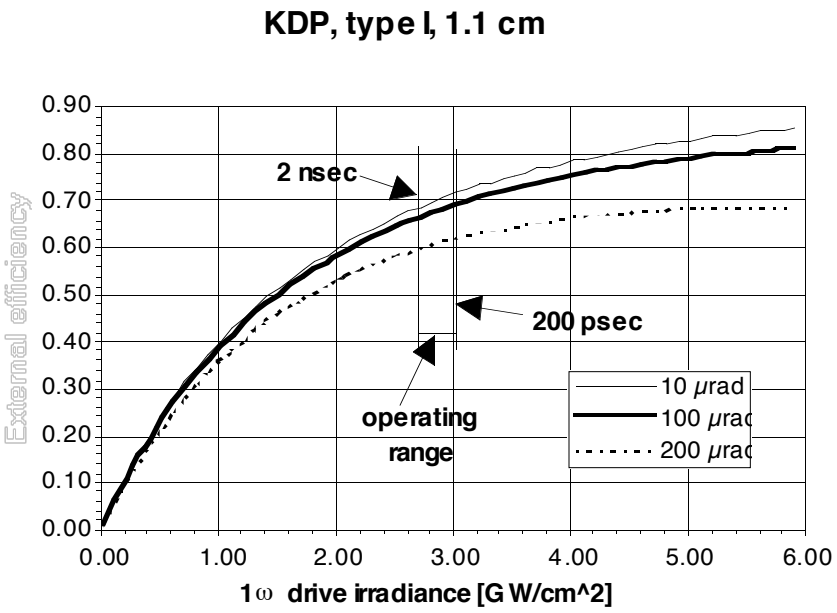

(a)

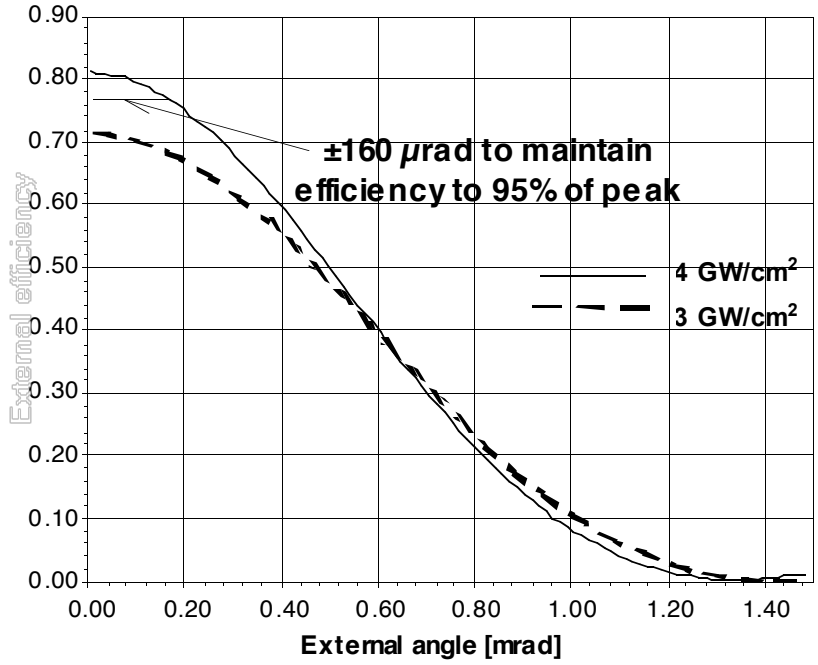

(b)

Figure 3-17. Calculated plane wave performance, baseline design.

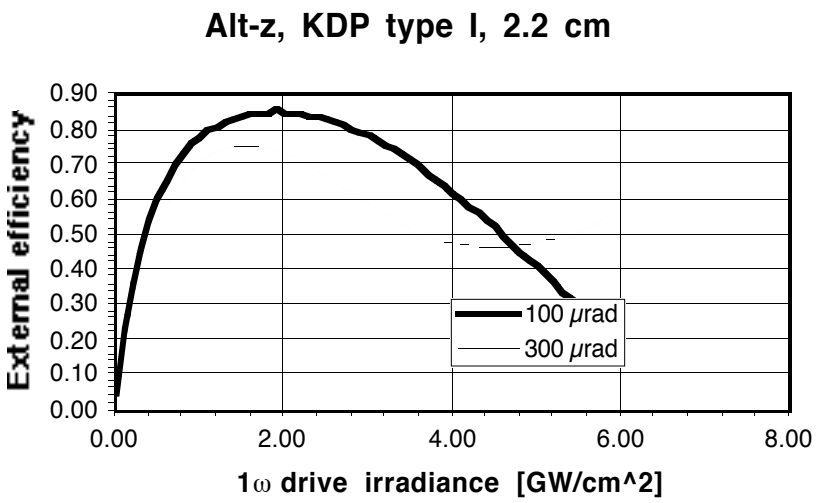

(a)

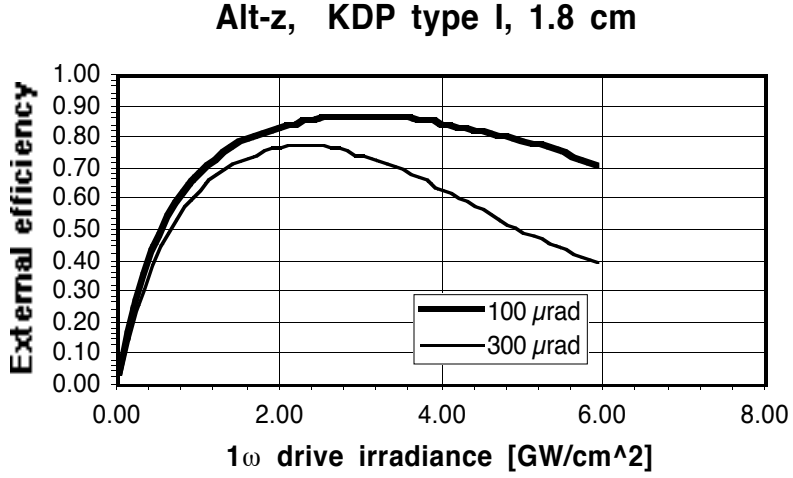

(b)

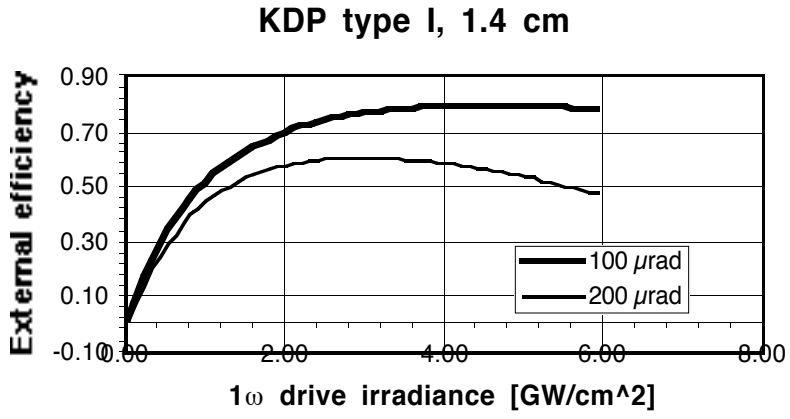

(c)

Figure 3-18. Calculated plane wave performance, advanced designs.

3.2.8 Site and Conventional Facilities—Design

Refer to **Figure 3-3** for the general layout of the interior of Building 986. Refer to **Figures 1-2** and **1-3** for site layout showing the relation between the Z-accelerator in Building 983 and the Backlighter in Building 986.

The site and conventional facilities modifications to Building 986 and Building 983 will be designed by SMPC Architects, a local commercial Architect/Engineering (A/E) firm under a fixed-price A/E master task contract. Construction will be accomplished by utilizing commercial construction contractors under a modified Firm-Fixed Price or Time and Materials contract, awarded on the basis of best value and/or competitive bid.

The overall scope of the modifications will be to convert the entire building (986) into a Class 100,000 clean room. This clean room will also be capable of supporting a smaller Class 100 modular clean room, several small mobile, modular Class 100 units, a control room and several gown rooms.

The Z-accelerator resides in the Building 983 high bay. No modifications to the Z-accelerator are required, although the building will require additional support towers adjacent to perimeter walls and wall penetrations for the transport tube.

The following is a list of some of the modifications to Building 986 that will be completed in order to accommodate the new operational requirements:

- Wall penetrations where the transport tube exits the building.
- Exterior foundations to support the transport tube and support frame.
- Exterior utility modifications to accommodate the foundation installations.
- Vibration isolation concrete pads at load locations.
- Utility trench with accessible covers.
- Exterior air lock/vestibule at northwest corner of building.
- Mezzanine to access mirrors at above floor locations.
- Class 100 modular clean room with gown room.
- Control room and MOR with gown room.
- Mylar-faced suspended ceiling panel system.
- HVAC chilled water system and support equipment.
- Air distribution ductwork system.
- Heated water system consisting of two gas fired boilers.
- Replace and/or repair of exterior doors and door frames.
- House vacuum system.
- Both low and high-pressure Nitrogen systems.
- Electrical panels, feeders, and branch circuits supplying interior power.
- Distribution switchboard system.
- Interior lighting system.
- Fire alarm system including duct smoke detectors, and audio/visual annunciation devices.

- Intrusion alarm system.
- Communication system.
- Lightning protection system.
- Grounding system.

Also, previously scheduled upgrades to the high-voltage power distribution system in Area 4 and the building's roof membrane will be coordinated to minimize disruption and downtime to the Backlighter Program. The high-voltage system was upgraded under the Power Systems Modernization (PSM) Project and the roof will be upgraded as part of the Sandia Maintenance Programs' routine repair, maintenance and renovation of building systems.

3.2.9 Laser Operations and Start-up

Operations

Based on a review of the technical support required for routine operation of the Nova and Beamlet facilities, we recommend that one staff scientist and three technicians be allocated to support Z-backlighter routine operations. The staff scientist should be responsible for assessment of laser and target physics issues, and supervision of the operations crew. Two of the technicians should be laser electro-optics technicians to support system operations; one additional technician with mechanical skills will be required to support clean-room operations. These technicians should work as a team with complete cross-training of operations and maintenance tasks. The setup and execution of routine shots should take 2–4 hours, allowing the remainder of the time to be used for system maintenance and repairs. The laser operators should be fully trained to support routine maintenance and repair tasks, including power conditioning, amplifier refurbishment, and optics installation. With effective cross-training this group should be adequate to support "normal" operations. Any unusual events, or off-normal operations may require additional support from existing Z-accelerator staff. Highly detailed or specialized electronics, computer, or mechanical repairs are expected to be supported by existing Z-accelerator staff qualified in the specific required technology. The proposed laser staff of four would be responsible for routine delivery of a beam to the output of the laser system, and the generation of x-rays in the target chamber. The primary interface with the main target chamber would be done by existing Z-accelerator staff and supported by the laser staff as required.

There will be a need to re-allocate existing custodial staff to maintain the cleanliness levels of the operations and support areas. This would require 1 to 2 people, for 8 hours, 2 to 3 times per week.

Well in advance of system installation and operation, it is recommended that the laser support technicians come to LLNL to work and train with Beamlet and Nova operations and maintenance personnel. This should include other electronics, computer, mechanical, and custodial staff as well. This will need to be addressed soon since the operating ICF laser facilities at LLNL will be shut down within the next year. Additionally, if new laser technicians need to be hired to fill these positions, the

recruiting and hiring process should begin soon, due to the limited availability of these technicians.

Some of the additional support (often done by LLNL personnel at LLNL test facilities) required for quality assurance of certain parts may be obtained from the vendors or in collaboration with LLNL. Such items include acceptance testing of flashlamps, and interferometry and photometry of certain optics.

Estimated funding required for routine procurements other than optics is detailed in **Table 3-7**. These estimates were extrapolated from current Nova and Beamlet operations. These costs are for routine operations and maintenance of the system. The allocation for optics processing includes an estimated cost of anti-reflection (A/R) coating debris shields at LLNL. The total annual cost of $170K compares well with the similar annual Beamlet budget of $228K, which covers a significantly larger number of shots per year.

Table 3-7. Estimated Z-backlighter Laser operating cost (thousands of dollars).

Supplies	Monthly	Annual	Nova
Optics Processing/Cleanroom	5	60	75
ME Operations	2	24	72
EE Operations (with flashlamps)	2	24	51
Controls/Data Acquisition	2	24	85
Facility Administration	1	12	36
MOR	1	12	116
Laser Operations	1	12	48
Alignment laser maintenance	0.2	2	36
Total Supplies / no optics	**14.2**	**170**	**519**

To estimate the annual cost of replacement optics for the Z-backlighter, we looked in detail at similar costs for routine operations of Nova. The relevant statistics for Nova are shown in **Table 3-8**. The optics listed represent the most vulnerable of the large optics in Nova in order to generate a conservative estimate. The spatial filter lens, for example, is the input lens to the final spatial filter, which sees the highest laser fluence. Since Nova fires about 3 times as many shots per year as required of the Z-backlighter, the last column of Table 3-7 indicates the expected use rate to be 33% of that experienced on Nova.

Table 3-8. Estimate of optics replacement rates based on Nova experience.

Optic	Use rate ($yr.^{-1}$)	Number in use	Use rate per optic	Use rate scaled to Z
31-cm disk re-polish	2	100	2%	0.7%
46-cm disk re-polish	3	160	2%	0.7%
31-cm polarizer	8	20	40%	13.0%
Spatial filter lens	6	10	60%	20.0%
31-cm mirrors	1	20	5%	1.7%
94-cm mirrors	3	45	7%	2.3%
Target chamber lenses	5	10	50%	17.0%
KDP crystals	3	10	30%	10.0%

An estimate of the annual cost of replacement optics for the Z-backlighter is given in **Table 3-9**. Each of the possible large optics procurements is listed in column 1 along with an estimate of its cost in column 2. The assumed use rate is a conservative value compared to Table 3-8. The estimated annual cost for each optic (column 5) is the product of columns 2, 3, and 4. In addition to the cost of large optics, there are a large number of small optics in the MOR, front-end, and diagnostic systems in the Z–Backligher. The number and complexity of these small optics is similar to that of the Nova MOR, so we estimate that the budget for small optics replacement should be equal to the annual budget of $30K for the Nova MOR. The total estimated cost for replacement optics for the Z-backlighter (sum of Table 3-9, column 5), not including debris shields, is $83K per year.

The largest single item cost of the Z-backlighter operations is assumed to be replacement of the debris shields, which are exposed to target debris. We make the conservative assumption that the debris shield will have to be replaced after every target shot. The cost of new debris shields, 30-cm in diameter, will be about $2000 each, so for 200 target shots/year the operating cost will be $400K. In practice we expect it will be possible to reuse some debris shields by repolishing one surface and applying new A/R coatings. If a large fraction of the debris shields can be reworked, it is possible that the $400K annual budget for replacement of debris shields could be reduced by one-half.

A summary of the total estimated operating costs for the Z-backlighter is shown in **Table 3-10**. Manpower for the staff scientist is estimated at $330K, while full-time operations technicians are estimated at $170K/year, including all general overhead and floor taxes. The bottom line indicates that an annual budget of $1.49M is to be expected.

Table 3-9. Z-backlighter optics replacement budget is estimated to be $83K per year.

Optics	Cost ($K)	Use rate	Number in use	Annual cost ($K)	Basis
40-cm disk blanks	provided	1%	11	—	Beamlet amplifier disks
40-cm disk re-polish	10	1%	11	1.1	Beamlet amplifier disks
Full aperture polarizer re-polish	5	15%	1	0.8	Nova 31-cm polarizer
Full aperture polarizer re-coat	7	15%	1	1.1	Nova 31-cm polarizer
Spatial filter lenses blanks	10	20%	6	12.0	Nova SF-7 lenses
Spatial filter lenses finish	7	20%	6	8.4	Nova SF-7 lenses
Full aperture mirrors re-polish	10	3%	7	2.1	Nova mirrors
Full aperture mirrors re-coat	25	3%	7	5.2	Nova mirrors
Pockels cell windows	20	20%	2	8.0	Nova SF-7 lenses
KDP crystals	20	10%	2	4.0	Nova converters
KDP re-polish	10	10%	2	2.0	Nova converters
Chamber window blanks	10	20%	1	2.0	Nova chamber lenses
Chamber window re-polish	7	20%	1	1.4	Nova chamber lenses
Chamber lens blanks	10	20%	1	2.0	Nova chamber lenses
Chamber lens re-polish	15	20%	1	3.0	Nova chamber lenses
Front/end diagnostics	small		many	30	Nova MOR
Optic Total per year				**$83K**	

Table 3-10. Z-backlighter laser operations will cost $1.49M/year including $400K for expendable debris shields.

Manpower (4 FTEs)	$840K
Operations and cleanroom	$170K
Optics replacement	$83K
Total excluding debris shields	$1,093K
Debris shields (200 @ $2K each)	$400K
Total operating expenses	$1.493M

FTE= Full-time employee

System Integration and Activation

This section provides a brief description of the steps required to integrate the laser subsystem and components and the complete activation of the laser system, and includes a preliminary description of the tests required to verify performance requirements. This activation is simplified by the fact that several subsystems are already in operation, previously used procedures can be applied, and benchmark performance data exist that can be used to verify proper installation and activation of the reassembled subsystem.

Figure 3-19 shows a schematic installation and activation flowchart and includes nearly all individual tasks to be accomplished before final system acceptance. Control system deployment is represented by the tasks in the left column. Their dependencies have been omitted in this diagram for the sake of clarity. Horizontally aligned activities are expected to take place concurrently.

The major activation milestone activities (highlighted in the diagram) are start-up of the MOR together with the timing system backbone, activation of the preamplifier and the alignment laser system, and activation of the main laser cavity and system diagnostics (up to and including the periscope mirrors and M_8 diagnostic splitter). Up to this point, activities are confined to the backlighter laser High Bay and no major impact on the operation of the accelerator is expected. However, during this time, impact of the Z-pinch firing on laser operations and alignment will have been evaluated. Although a formal integration of the backlighter and Z control system is not required during this time, early integration experience would be beneficial to allow sufficient time to gain operational experience and fine-tune control software.

Once the 1ω laser system has been activated and characterized at nominal performance levels, the frequency doubler will be activated, followed by doubling performance characterization and finally transporting the beam to the final optics and target chamber. After initial pointing and timing tests, the system is ready to test performance, initially at high power using short pulses (<200 ps) at safe fluence levels, followed by acceptance tests using backlighter targets and appropriate x-ray imaging, spectral and timing diagnostics.

Once durations, resources, and interactions have been assigned to the individual activation and installation activities, the logic flowchart will serve as the basis for a detailed PERT analysis and schedule for the backlighter start-up.

LLNL laser scientists will train and assist Sandia operators in the laser setup operation, diagnostic alignment and maintenance, troubleshooting, and repair. System performance margins will be evaluated for the expected range of laser pulse durations and shapes, and laser propagation codes will be made available to allow safe setup of the system operating conditions by the operators. After initial operation, a system check of all system optics will be performed to verify that appropriate cleanliness was maintained during installation, and no significant effect of hydrocarbons on sol-gel coatings exists.

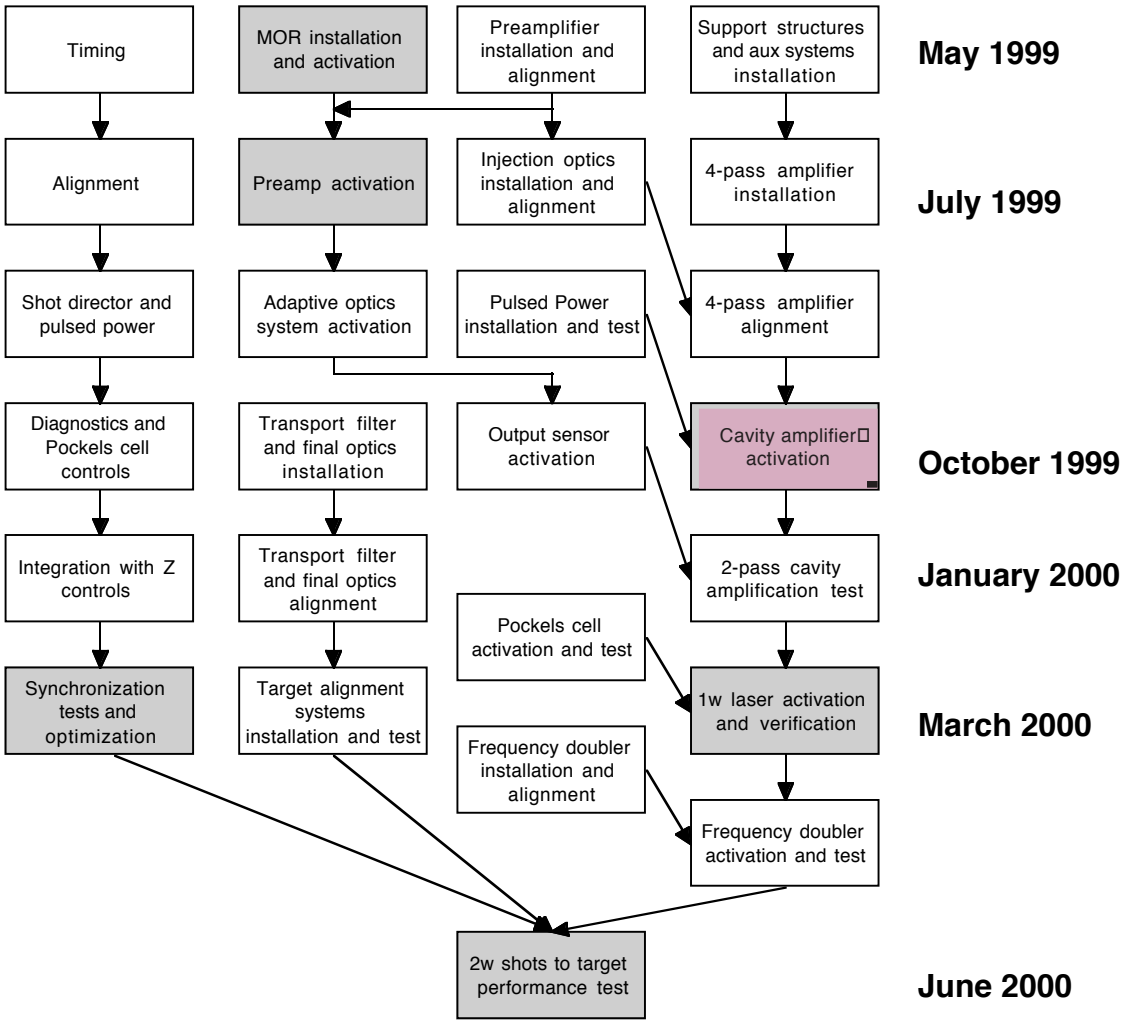

Figure 3-19. Z-backlighter Laser installation and activation flowchart.

4.0 Schedule

The schedule for completion of the Z-backlighter Laser Initiative is shown in **Figure 4-1**. A critical aspect of the schedule is the need to make a commitment early in FY99 to doing the required facility modifications, and to initiate long lead time procurements. The Building 986 facility renovation must be complete by June 1999 in order to maintain the schedule.

Components from Beamlet were disassembled and stored starting in Q4 FY98, and installation and re-activation at Sandia can begin as soon as the Building 986 laser facility is available. The Z-backlighter front-end will be operational by November 1999.

Installation of the Beamlet cavity amplifiers must be completed by Q1 FY00, so that 1ω test shots can be fired early in Q2 FY00. This will be followed by a series of tests of the interaction and synchronization of the Z-Beamlet laser and the Z-accelerator.

Activation of the frequency conversion system and 2ω performance tests will precede final activation of the laser system in Q3 FY00. Given the proposed aggressive funding profile (Figure 1-4), the system will be operational on June 30, 2000. We anticipate that the exact schedule can and will be modified based on the availability of funds.

ID	Task Name
1	Advanced conceptual design and risk reduction
2	A-CDR publication and review
3	DOE authorization received
4	Facility design contract (Bldg. 966)
5	Facility design review
6	Laser facility construction
7	966 MOR and control room ready
8	Class 100,000 laser bay certification
9	Front end capacitor bank installation
10	Control Room server installation and activation
11	Front end cap bank & control activation
12	MOR installation
13	Front end installation and activation
14	Front end operational
15	Main capacitor bank installation and activation
16	Pulsed power controls installation and activation
17	Class 100 clean room installation and activation
18	Class 100 clean room operational
19	Cavity amplifier assembly and installation
20	Test fire amplifier flashlamps
21	Cavity amplifiers operational
22	Cavity spatial filter modification and installation
23	PEPC assembly and installation
24	Bridge, TSF and periscope optics installation
25	1w alignment/diagnostic & controls install and activate
26	1w performance tests
27	1w performance verified
28	Install frequency converter
29	2w alignment/diagnostic & controls install and activate
30	2w performance tests
31	2w performance verified
32	986-983 Breeze-way construction
33	2w relay telescope installation
34	2w calorimeter and beam tube installation
35	Final optics installation and alignment
36	Backlighter target installation and alignment
37	2w shots on target w/o & w/ Z-accelerator shot
38	Z-backlighter system operational

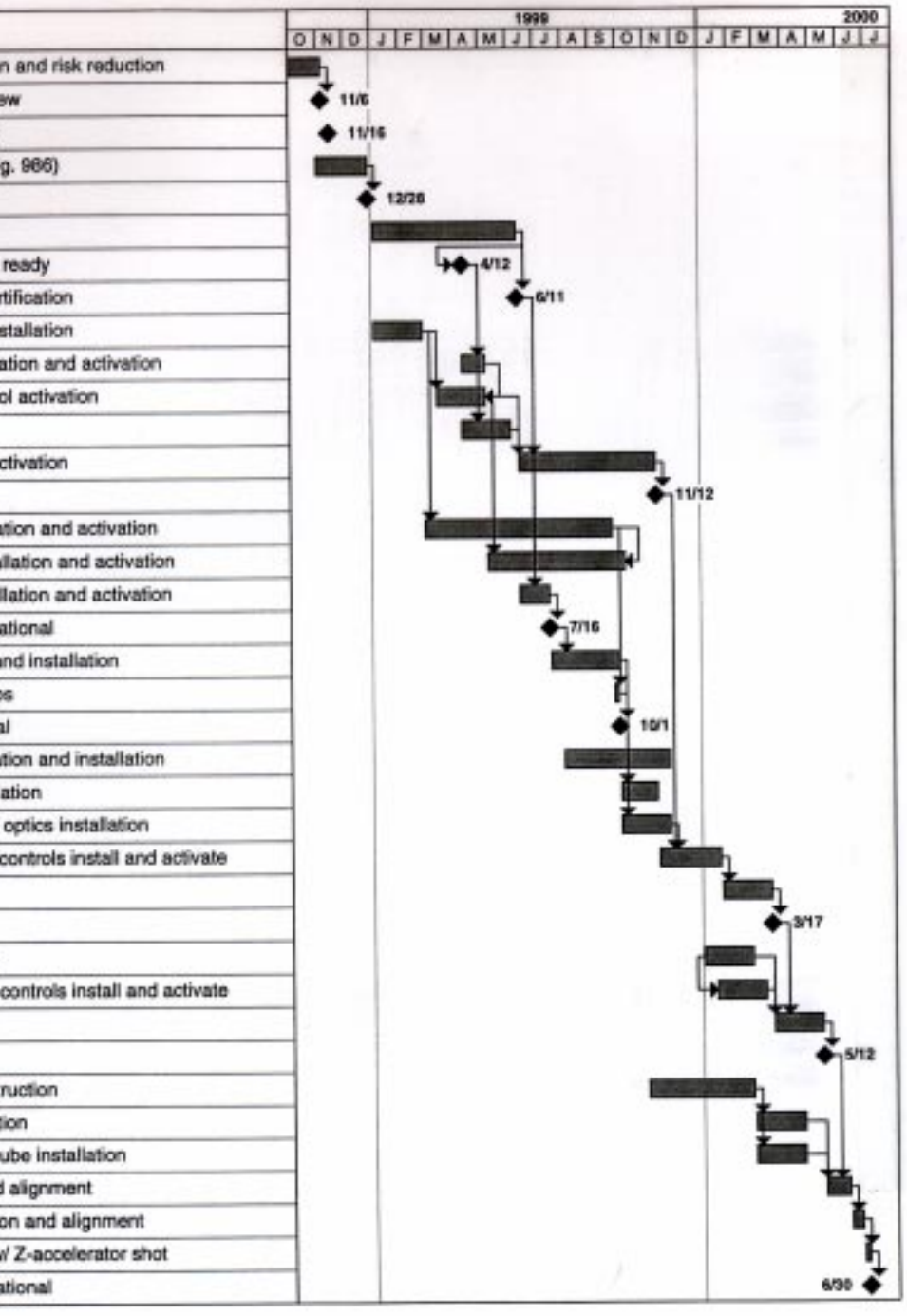

Task
Progress
Milestone
Summary
Rolled Up Task
Rolled Up Milestone
Rolled Up Progress
External Tasks
Project Summary
Split
Rolled Up Split

Figure 4-1. Proposed Z-Backlighter Schedule.

References

1. B. M. Van Wonterghem, J. R. Murray, J. H. Campbell, D. R. Speck, C. E. Barker, I. C. Smith, D. F. Browning, and W. C. Behrendt, "Performance of a prototype for a large-aperture multi-pass Nd:glass laser for inertial confinement fusion," *Applied Optics*, vol. 36, pp. 4932-4953 (1997).
2. M. A. Rhodes, B. Woods, J. J. De Yoreo, D. Roberts, and L. J. Atherton, "Performance of large-aperture optical switches for high-energy inertial-confinement fusion lasers," *Applied Optics*, vol. 34, pp. 5312-5325 (1995).
3. J. Goldhar and M. Henesian, "Large-aperture electro-optical switches with plasma electrodes," *IEEE J. Quantum Electronics*, vol. QE-22, pp. 1137-1147 (1986).
4. P. J. Wegner, B. M. Van Wonterghem, S. N. Dixit, M. A. Henesian, C. E. Barker, C. E. Thompson, L. G. Seppala, and J. A. Caird, "Characterization of third-harmonic target plane irradiance on the National Ignition Facility Beamlet Demonstration Project," presented at the 12th Topical Meeting on the Technology of Fusion Energy, Reno, NV, June, 1996.
5. P. Wegner and B. Van Wonterghem, "Measurements of Beamlet wavefront divergence," Lawrence Livermore National Laboratory, internal memorandum, LST-BLT97-068, April 29, 1997.
6. U.S. Department of Energy, "Natural Phenomena Hazards Design and Evaluation Criteria for Department of Energy Facilities," Washington, D.C., DOE-STD-1020, January 1996.
7. S.C. Sommer, "NIF Broadband and Narrowband Vibration Criteria", NIF-0004049, Lawrence Livermore National Laboratory, Livermore, California, December 1, 1997.
8. S.C. Sommer, "Methodology for stability flowdown for Z-backlighter Project," informal memorandum, Lawrence Livermore National Laboratory, Livermore, California, September 23, 1997.
9. S.C. Sommer and D.W. Coats, "Wind Provisions for NIF", NIF-0002800-OA, Lawrence Livermore National Laboratory, Livermore, California, July 23, 1997.
10. R. A. Sacks, M. A. Henesian, S. W. Haney, and J. B. Trenholme, "The PROP92 Fourier Beam Propagation Code," *ICF Quarterly Report*, Vol. 6, #4, LLNL Report UCRL-LR-105821-96-4 (July-Sept. 1996), p. 207.
11. F. Rainer, F. P. DeMarco, M. C. Staggs, M. R. Kozlowski, L. J. Atherton, and L. M. Sheehan, "A Historical Perspective on Fifteen Years of Laser Damage Thresholds at LLNL," Lawrence Livermore National Laboratory Report UCRL-JC-114997 prepared for the 1993 Boulder Damage Symposium, Boulder, Colorado, October 27–29, 1993; and F. Rainer, J. Atherton, M. Kozlowski, "Current and Projected Damage Thresholds for NIF Optical Components," LLNL Report LDG 93-033 (June 21, 1993). Both the HR threshold at 1ω and the polarizer reflection threshold at 1ω were reduced below the thresholds used previously for the NIF design, to match the data for existing Beamlet parts (private communication, Chris Stolz).
12. C. D. Orth, S. W. Haney, and W. H. Williams, "Laser Optimization Techniques," *ICF Quarterly Report*, Vol. 6, #4, LLNL Report UCRL-LR-105821-96-4 (July-Sept. 1996), p. 192.

13. H. Patton, "PBFA Input," Lawrence Livermore National Laboratory, Livermore, California, July 2, 1997.
14. P.S. Barney, "Z-pinch Phase C Room Floor Survey," Sandia National Laboratories, Albuquerque, New Mexico, November 19, 1997.
15. P.S. Barney, "Z-pinch Phase C Room Floor Survey," Sandia National Laboratories, Albuquerque, New Mexico, December 17, 1997.
16. S.C. Sommer, "Methodology for stability flowdown for Z-backlighter Project," informal memorandum, Lawrence Livermore National Laboratory, Livermore, California, September 23, 1997.
17. R. Berger, "Class 10,000 & Class 100 Clean Facilities," Brycon Corporation, Rio Rancho, New Mexico, December 18, 1997.